Thermodynamic Properties of *o*-Xylene, *m*-Xylene, *p*-Xylene, and Ethylbenzene

Yong Zhou (周永)

*MOE Key Laboratory of Thermo-Fluid Science and Engineering, Xi'an Jiaotong University, Xi'an Shaanxi 710049,
People's Republic of China, and Thermophysical Properties Division, National Institute of Standards and Technology,
325 Broadway, Boulder, Colorado 80305, USA*

Jiangtao Wu (吴江涛)

*MOE Key Laboratory of Thermo-Fluid Science and Engineering, Xi'an Jiaotong University, Xi'an Shaanxi 710049,
People's Republic of China*

Eric W. Lemmon[a]

*Thermophysical Properties Division, National Institute of Standards and Technology, 325 Broadway, Boulder,
Colorado 80305, USA*

Equations of state for the xylene isomers (*o*-xylene, *m*-xylene, and *p*-xylene) and ethylbenzene have been developed with the use of the Helmholtz energy as the fundamental property with independent variables of density and temperature. The general uncertainties of the equations of state are 0.5% in vapor pressure above the normal boiling point, and increase as the temperature decreases due to a lack of experimental data. The uncertainties in density range from 0.1% in the liquid region to 1.0% elsewhere (the critical and vapor-phase regions). The uncertainties in properties related to energy (such as heat capacity and sound speed) are estimated to be 1.0%. In the critical region, the uncertainties are higher for all properties. The behavior of the equations of state is reasonable within the region of validity and at higher and lower temperatures and pressures. Detailed analyses between the equations and experimental data are reported. © *2012 by the U.S. Secretary of Commerce on behalf of the United States. All rights reserved.* [http://dx.doi.org/10.1063/1.3703506]

Key words: equation of state; ethylbenzene; *m*-xylene; *o*-xylene; *p*-xylene; xylene isomers.

CONTENTS

List of Tables

[a] Author to whom correspondence should be addressed; Electronic mail: eric.lemmon@nist.gov; Fax: (303) 497-5044.

List of Figures

List of Symbols

a = specific Helmholtz energy
a_i, n_i, υ_i = coefficient
B = second virial coefficient
c_p = specific isobaric heat capacity
c_v = specific isochoric heat capacity
c_σ = specific saturation heat capacity
$d_i, l_i, t_i, u_i, \beta_i, \gamma_i, \varepsilon_i, \eta_i$ = exponents
e = specific internal energy
h = specific enthalpy
i = serial number
k_s = isentropic expansion coefficient
k_T = isothermal expansion coefficient
N = number of data points

p = pressure
R = molar gas constant
s = specific entropy
T = temperature
v = specific volume
w = sound speed
Z = compression factor

Greek Letters

Δ = deviation
α = dimensionless Helmholtz energy
α_v = volume expansivity
γ = Gruneisen coefficient
δ = reduced density
ρ = density
τ = inverse reduced temperature

Superscripts

0 = ideal-gas
r = residual
$'$ = saturated liquid state

Subscripts

0 = reference state property
c = critical
calc = calculated
exp = experimental
max = maximum
min = minimum
tp = triple-point property
σ = saturation property

1. Introduction

1.1. Characteristics of xylene isomers and ethylbenzene

Xylene is a specific term that represents the three isomers of dimethyl benzene—these isomers are the *ortho*-, *meta*-, and *para*- forms of the molecule. Ethylbenzene is the fourth and only other isomer of this benzene molecule, with an additional ethyl group. Figure 1 shows the chemical structure of the xylene isomers and of ethylbenzene, and Table 1 gives additional information such as the critical points and molar masses.

Xylene isomers are of great importance in the petrochemical industry because they are the basis for the synthesis of many organic compounds.[1] *o*-Xylene is mainly used for production of *o*-dicarboxylic anhydride, which is an important raw material and widely used in plasticizers, unsaturated polyester, alkyd resins, dyes, medicine, and agriculture. *m*-Xylene is used to produce isophthalic acid, which is an
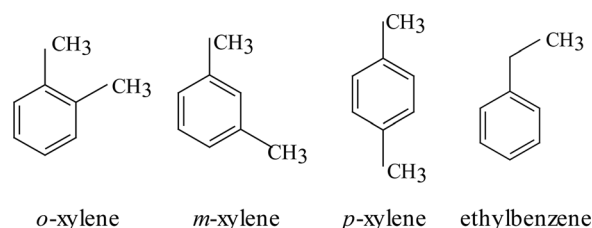
FIG. 1. The chemical structure of *o*-xylene, *m*-xylene, *p*-xylene, and ethylbenzene.

important material in dyes, pesticides, chemical fibers, spices, and other industries. *p*-Xylene is an important organic chemical that is mainly used to synthesize terephthalate, while terephthalate is the main raw material used to produce resins, films, and other products. Another application of *p*-xylene is the production of dimethyl terephthalate.[2] Ethylbenzene is important in the petrochemical industry as an intermediate in the production of styrene, which in turn is used for making polystyrene—a common plastic material.[3]

Xylenes are normally produced as a mixed stream that contains *o*-xylene, *m*-xylene, *p*-xylene, and ethylbenzene. It is difficult to separate the C8 aromatic compounds—this process has more than 200 stages due to the low relative volatilities of the compounds and the high degree of purity required for the final products.[4] Hence, thermodynamic properties are required to simulate and optimize the separation process, along with many other industrial applications.

1.2. Equation of state

Thermodynamic properties of pure fluids and their mixtures can be calculated with equations of state. These equations are expressed as either the pressure as a function of independent variables temperature and density, or as the Helmholtz energy with the same independent variables. The Helmholtz energy equation has the advantage that all thermodynamic properties can be derived easily from the equation of state.[5] The calculation of thermodynamic properties from the Helmholtz energy equation of state is described in many publications, such as those of Wagner and Pruß,[6] Span,[7] or Lemmon *et al*.,[5] and these concepts are not repeated here.

1.3. Critical parameters of xylene isomers and ethylbenzene

The critical parameters are some of the most important substance-specific constants in thermodynamics, in part because they are used as reducing parameters in many equations of state, viscosity equations, thermal conductivity equations, and other auxiliary equations. The critical parameters can be very difficult to measure, often with large differences between various sources. The published critical parameters are listed in Table 2 along with the values chosen in this work. Many of these were obtained through the ThermoData Engine (TDE) (Ref. 32) program of NIST. We used the evaluated critical temperatures and densities taken from TDE to develop the equations of state in this work. Due to the lack

TABLE 1. Identifications and fundamental constants of o-xylene, m-xylene, p-xylene, and ethylbenzene

Short Name	o-xylene	m-xylene	p-xylene	ethylbenzene
CAS number	95-47-6	108-38-3	106-42-3	100-41-4
Full name	1,2-dimethylbenzene	1,3-dimethylbenzene	1,4-dimethylbenzene	Phenylethane
Chemical formula		C_8H_{10}		
Molar mass (g mol^{-1})		106.165		
Triple-point temperature (K)	247.985	225.3	286.4	178.2
Critical temperature (K)	630.259	616.89	616.168	617.12
Critical density (mol dm^{-3})	2.6845	2.665	2.69392	2.741016
Critical pressure (kPa)	3737.5	3534.6	3531.5	3622.4
Normal boiling point (K)	417.521	412.214	411.47	409.314
Acentric factor	0.312	0.326	0.324	0.304

of experimental p-ρ-T data with low uncertainties in the critical region, it was not possible to verify the uncertainties of these values, as was done with other fluids such as propane.[5] The critical pressures given in Tables 1 and 2 were determined with the final equations of state.

2. Equation of State

The equation of state is formulated with the Helmholtz energy as the fundamental property with independent variables density and temperature. The equation is given by

$$a(\rho, T) = a^0(\rho, T) + a^r(\rho, T), \tag{1}$$

where a is the Helmholtz energy, a^0 is the ideal-gas Helmholtz energy, and a^r is the residual Helmholtz energy. All thermodynamic properties can be calculated as derivatives of the Helmholtz energy; see Ref. 5 for details. The most commonly used functional form is explicit in the dimensionless

Helmholtz energy with independent variables of dimensionless density and temperature, as

$$\frac{a(\rho, T)}{RT} = \alpha(\delta, \tau) = \alpha^0(\delta, \tau) + \alpha^r(\delta, \tau), \tag{2}$$

where $\delta = \rho/\rho_c$ and $\tau = T_c/T$. The critical temperatures and densities used as the reducing parameters for the equations of state developed here are listed in Tables 1 and 2.

The dimensionless form of the ideal-gas Helmholtz energy equation can be represented by

$$\alpha^0(\delta, \tau) = \frac{h_0^0 \tau}{RT_c} - \frac{s_0^0}{R} - 1 + \ln\frac{\delta\tau_0}{\delta_0\tau} - \frac{\tau}{R}\int_{\tau_0}^{\tau}\frac{c_p^0}{\tau^2}d\tau + \frac{1}{R}\int_{\tau_0}^{\tau}\frac{c_p^0}{\tau}d\tau, \tag{3}$$

where $\delta_0 = \rho_0/\rho_c$, $\tau_0 = T_c/T_0$, and T_0, ρ_0, h_0^0, and s_0^0 are used to define an arbitrary reference state point. As defined by Eq. (3), the calculation of thermodynamic properties with an equation of state explicit in the Helmholtz energy is obtained from the use of an equation for the ideal-gas heat

TABLE 2. Summary of critical parameters for o-xylene, m-xylene, p-xylene, and ethylbenzene

Author	Year	Critical temperature (K)	Critical pressure (kPa)	Critical density (mol dm^{-3})
		o-Xylene		
Altschul[8]	1893	631.485	3618.65	
Brown[9]	1906	636.135		
Fischer and Reichel[10]	1943	631.685		
Ambrose and Grant[11]	1957	630.285		
Francis[12]	1957	631.185		
Glaser and Ruland[13]	1957	617.487		
Simon[14]	1957	631.085		2.71
Richardson and Rowlinson[15]	1959	629.385		
Ambrose et al.[16]	1967		3733	
Kay and Hissong[17]	1967	630.185	3715.57	
Akhundov and Imanov[18]	1970			2.6986
Mamedov et al.[19]	1970	631.548	3808.1	
Ambrose[20]	1987	630.288	3731.8	
Christou[21]	1988	630.258		
Chirico et al.[22]	1997	630.5		
This work	**2011**	**630.259 ± 0.1**	**3737.5 ± 30**	**2.6845 ± 0.3**

TABLE 2. Summary of critical parameters for *o*-xylene, *m*-xylene, *p*-xylene, and ethylbenzene—Continued

Author	Year	Critical temperature (K)	Critical pressure (kPa)	Critical density (mol dm^{-3})
m-Xylene				
Altschul[8]	1893	618.786	3510.78	
Brown[9]	1906	622.186		
Ambrose and Grant[11]	1957	616.487		
Francis[12]	1957	620.186		
Glaser and Ruland[13]	1957	617.487		
Simon[14]	1957	616.787		
Ambrose et al.[16]	1967	617.007	3541	
Akhundov and Asadullaeva[23]	1968			2.68356
Ambrose[20]	1987	617.009	3541.2	
Christou[21]	1988	617.059		
Chirico et al.[22]	1997	617.6		2.66566
This work	**2011**	**616.89 ± 0.3**	**3534.6 ± 20**	**2.665 ± 0.1**
p-Xylene				
Altschul[8]	1893	617.587	3432.33	
Brown[9]	1906	621.682		
Fischer and Reichel[10]	1943	618.187		
Ambrose and Grant[11]	1957	616.187		
Francis[12]	1957	619.186		
Glaser and Ruland[13]	1957	617.487		
Simon[14]	1957	615.937		2.644
Ambrose et al.[16]	1967		3511	
Akhundov and Imanov[18]	1970			2.661
Mamedov et al.[19]	1970	618.109	3617.5	
Powell et al.[24]	1970	616.159	3510.7	
Ambrose[20]	1987	616.189		
Christou[21]	1988	616.159		
Chirico et al.[22]	1997	616.4		
This work	**2011**	**616.168 ± 0.1**	**3531.5 ± 20**	**2.69392 ± 0.3**
Ethylbenzene				
Altschul[8]	1893	619.586	3736.33	
Simon[14]	1957	617.187		2.67037
Ambrose et al.[25]	1960	617.157		
Ambrose et al.[16]	1967	617.107	3609	
Kay and Hissong[17]	1967	617.487	3616.98	
Kay and Hissong[26]	1969	616.709	3619.06	
Raetzsch and Strauch[27]	1972	618.159		
Ambrose[20]	1987	617.159	3608.3	
Wilson et al.[28]	1995	617.26	3616	2.69398
Chirico et al.[29]	1997	617.3		
Von Niederhausern et al.[30]	2000	618	3620	
Nikitin et al.[31]	2002	614	3600	
This work	**2011**	**617.12 ± 0.1**	**3622.4 ± 15**	**2.741016 ± 0.4**

capacity, c_p^0. Since there are no experimental ideal-gas heat-capacity data available, the values were estimated by a group contribution method[33] and are fitted to the equation,

$$\frac{c_p^0}{R} = v_0 + \sum_{i=1}^{I_{\text{Ideal}}} v_i \left(\frac{u_i}{T}\right)^2 \frac{\exp(u_i/T)}{[\exp(u_i/T) - 1]^2}, \quad (4)$$

where $R = 8.314\ 472$ J mol^{-1} K^{-1} is the molar gas constant,[34] and I_{Ideal} is 4 for *o*-xylene, *m*-xylene, and *p*-xylene, and 3 for ethylbenzene. The coefficients and exponents of

the ideal-gas heat capacity equations are given in Table 3. A more convenient form of the ideal-gas Helmholtz energy, derived from the integration of Eq. (3) and the application of a reference state with zero enthalpy and entropy at the normal boiling point for the saturated liquid, is

$$\alpha^0 = \ln \delta + (v_0 - 1) \ln \tau + a_1 + a_2 \tau$$
$$+ \sum_{i=1}^{I_{\text{Ideal}}} v_i \ln \left[1 - \exp\left(\frac{-u_i \tau}{T_c}\right)\right], \quad (5)$$

where a_1 and a_2 are given in Table 4.

TABLE 3. Coefficients and exponents of the ideal-gas heat-capacity equations

i	v_i	u_i (K)	v_i	u_i (K)
		o-Xylene	m-Xylene	
0	3.748798	–	2.169909	–
1	4.754892	225	4.443120	160
2	6.915052	627	2.862794	190
3	25.84813	1726	24.83298	1333
4	10.93886	4941	16.26077	3496
		p-Xylene	Ethylbenzene	
0	5.2430504	–	5.2557889	–
1	5.2291378	414	9.7329909	585
2	19.549862	1256	11.201832	4420
3	16.656178	2649	25.440749	1673
4	5.9390291	6681		

TABLE 4. Coefficients of the ideal-gas Helmholtz energy equation

	a_1	a_2
o-Xylene	10.137376	−0.91282993
m-Xylene	12.652887	−0.45975624
p-Xylene	5.9815241	−0.52477835
Ethylbenzene	5.7040900	−0.52414353

The real-fluid behavior is often described with empirical models, and any functional connection to theory is not entirely justified. The coefficients of the equation depend on the experimental data for the fluid and are constrained by various criteria.[35] In the development of an equation of state, the data are carefully evaluated, and the behavior of the equation is viewed graphically to ensure reasonable behavior in the absence of experimental data over the full surface of the fluid. The functional form for the residual Helmholtz energy is

$$\alpha^{\mathrm{r}}(\delta,\tau) = \sum_{i=1}^{I_{\mathrm{Pol}}} n_i \delta^{d_i} \tau^{t_i} + \sum_{i=I_{\mathrm{Pol}}+1}^{I_{\mathrm{Pol}}+I_{\mathrm{Exp}}} n_i \delta^{d_i} \tau^{t_i} \exp\left(-\delta^{l_i}\right)$$
$$+ \sum_{i=I_{\mathrm{Pol}}+I_{\mathrm{Exp}}+1}^{I_{\mathrm{Pol}}+I_{\mathrm{Exp}}+I_{\mathrm{GBS}}} n_i \delta^{d_i} \tau^{t_i} \exp\left(-\eta_i(\delta-\varepsilon_i)^2 - \beta_i(\tau-\gamma_i)^2\right).$$

$$(6)$$

where the values of t_i should be greater than zero, and d_i and l_i should be integers greater than zero. The coefficients and

exponents of the residual part of the equations of state are given in Tables 5 and 6. The ranges of validity are shown in Table 7. As analyzed in Sec. 3, the equations of state developed here have reasonable extrapolation behavior; the equations can be used over a much broader range of conditions, with temperatures up to the limit of decomposition and pressures up to two times the values given in Table 7.

In the following sections, the percent deviation between the experimental data and values calculated by the equation of state for any property, X, is defined as

$$\%\Delta X = 100\left(\frac{X_{\mathrm{exp}} - X_{\mathrm{calc}}}{X_{\mathrm{exp}}}\right). \qquad (7)$$

With this definition, the average absolute deviation (AAD) and Bias are defined as

$$\mathrm{AAD} = \frac{1}{N_{\mathrm{exp}}} \sum_{i=1}^{N_{\mathrm{exp}}} |\%\Delta X_i|, \qquad (8)$$

and

$$\mathrm{Bias} = \frac{1}{N_{\mathrm{exp}}} \sum_{i=1}^{N_{\mathrm{exp}}} (\%\Delta X_i), \qquad (9)$$

where N_{exp} is the number of data points. In the figures discussed below, symbols shown at the top or bottom of the

TABLE 5. Coefficients and exponents of the equations of state

i	n_i	t_i	d_i	l_i	n_i	t_i	d_i	l_i
		o-Xylene				m-Xylene		
1	0.0036765156	1	5		0.000012791017	1	8	
2	−0.13918171	0.6	1		0.041063111	0.91	4	
3	0.014104203	0.91	4		1.505996	0.231	1	
4	1.5398899	0.3	1		−2.3095875	0.772	1	
5	−2.3600925	0.895	1		−0.46969	1.205	2	
6	−0.44359159	1.167	2		0.171031	0.323	3	
7	0.19596977	0.435	3		−1.001728	2.7	1	2
8	−1.0909408	2.766	1	2	−0.3945766	3.11	3	2
9	−0.21890801	3.8	3	2	0.6970578	0.768	2	1
10	1.1179223	1.31	2	1	−0.3002876	4.1	2	2
11	−0.93563815	3	2	2	−0.024311	0.818	7	1
12	−0.018102996	0.77	7	1	0.815488	2	1	
13	1.4172368	1.41	1		−0.330647	2.9	1	
14	−0.57134695	4.8	1		−0.123393	3.83	3	
15	−0.081944041	1.856	3		−0.54661	0.5	3	
16	−40.682878	2	3					

Table 5. Coefficients and exponents of the equations of state—Continued

i	n_i	t_i	d_i	l_i	n_i	t_i	d_i	l_i
		p-Xylene				Ethylbenzene		
1	0.0010786811	1.	5		0.0018109418	1	5	
2	−0.103161822	0.83	1		−0.076824284	1	1	
3	0.0421544125	0.83	4		0.041823789	0.92	4	
4	1.47865376	0.281	1		1.5059649	0.27	1	
5	−2.4266	0.932	1		−2.4122441	0.962	1	
6	−0.46575193	1.1	2		−0.47788846	1.033	2	
7	0.190290995	0.443	3		0.18814732	0.513	3	
8	−1.06376565	2.62	1	2	−1.0657412	2.31	1	2
9	−0.209934069	2.5	3	2	−0.20797007	3.21	3	2
10	1.25159879	1.2	2	1	1.1222031	1.26	2	1
11	−0.951328356	3	2	2	−0.99300799	2.29	2	2
12	−0.0269980032	0.778	7	1	−0.027300984	1	7	1
13	1.37103180	1.13	1		1.3757894	0.6	1	
14	−0.494160616	4.5	1		−0.44477155	3.6	1	
15	−0.0724317468	2.2	3		−0.07769742	2.1	3	
16	−3.69464746	2	3		−2.16719	0.5	3	

plot represent data with deviations greater than the minimum or maximum values on the y-axis.

2.1. Equation of state for *o*-xylene

Experimental data for *o*-xylene are summarized in Table 8, and the AADs between experimental data and values calculated with the equation of state are listed in the last column. Part of the data reported here were obtained from the TDE (Ref. 32) of the Thermodynamics Research Center (TRC) of

Table 6. Coefficients of the equations of state

i	η_i	β_i	γ_i	ε_i
		o-Xylene		
13	1.1723	2.442	1.2655	0.552
14	1.095	1.342	0.3959	0.728
15	1.6166	3	0.7789	0.498
16	20.4	450	1.162	0.894
		m-Xylene		
12	1.0244	1.66	1.1013	0.713
13	1.3788	1.9354	0.6515	0.9169
14	0.9806	1.0323	0.4975	0.6897
15	6.3563	78	1.26	0.7245
		p-Xylene		
13	1.179	2.445	1.267	0.54944
14	1.065	1.483	0.4242	0.7234
15	1.764	4.971	0.864	0.4926
16	13.675	413	1.1465	0.8459
		Ethylbenzene		
13	1.178	2.437	1.2667	0.5494
14	1.07	1.488	0.4237	0.7235
15	1.775	4	0.8573	0.493
16	15.45	418.6	1.15	0.8566

NIST, and the rest from the open literature. Data sets with only one to four data points were combined and labeled as "other data sets," except for those that were important to the development of the equations of state.

Figure 2 presents comparisons of vapor pressures for *o*-xylene calculated with the equation of state to experimental data. The equation represents vapor pressures generally within 0.5% above 300 K. There is a large number of experimental data for the normal boiling point; the deviations of most are within 1.0%, and the equation of state passes through the center of the data. The values reported by Willingham *et al.*[40] and Chirico *et al.*[22] are quite similar below the normal boiling temperature, and the data reported by Ambrose *et al.*,[16] Mamedov *et al.*,[19] and Ambrose[20] agree very well at higher temperatures. Because of the disagreement between the data of Chirico *et al.*[22] and Ambrose[20] near 450 K, it is not possible to fit the higher-temperature data to better than 0.2%. Below 300 K, the data are dissimilar, with no reliable values that can be used to fit the equation.

Figure 3 gives comparisons of saturated liquid densities calculated with the equation of state to experimental data. The equation represents much of the data to within 0.1% below 500 K. There are many values between 290 K and 300 K, mostly from single sources. The majority of these are fit within 0.05%, and we fitted the equation to the mean of

Table 7. The range of validity of the equations

	o-Xylene	*m*-Xylene	*p*-Xylene	Ethylbenzene
T_{min} (K)	247.985	225.3	286.4	178.2
T_{max} (K)	700	700	700	700
p_{max} (MPa)	70	200	200	60
ρ_{max} (mol dm^{-3})	8.648	8.677	8.166	9.124

TABLE 8. Summary of experimental data for *o*-xylene

Author	Number of points	Temperature range (K)	Pressure range (MPa)	AAD (%)	Bias (%)
		Vapor pressure			
Neubeck (1887)[36]	9	364–416	0.02–0.101	3.942	3.942
Woringer (1900)[37]	30	273–418	0.001–0.105	23.079	23.079
Kassel (1936)[38]	9	273–353	0–0.013	10.214	10.214
Pitzer and Scott (1943)[39]	6	273–333	0–0.005	1.206	−1.206
Willingham *et al.* (1945)[40]	20	337–418	0.006–0.104	0.055	−0.053
Forziati *et al.* (1949)[41]	20	337–419	0.006–0.104	0.061	−0.058
Glaser and Ruland (1957)[13]	17	417–613	0.101–3.04	0.988	−0.223
Ambrose *et al.* (1967)[16]	8	480–620	0.414–3.3	0.107	−0.036
Mamedov *et al.* (1970)[19]	38	448–632	0.215–3.81	0.240	0.160
Nigam and Mahl (1971)[42]	6	293–303	0.001	1.657	−1.657
Diaz Peña *et al.* (1979)[43]	5	333–353	0.005–0.013	0.190	0.190
Castellari *et al.* (1982)[44]	6	386–416	0.04–0.099	1.606	−0.263
Hessler and Lichtenstein (1986)[45]	19	248–283	3.38×10^{-5}–3.24×10^{-4}	12.036	6.940
Ambrose (1987)[20]	39	432–620	0.146–3.32	0.122	−0.052
Chirico *et al.* (1997)[22]	23	313–459	0.002–0.27	0.024	−0.016
Rodrigues *et al.* (2005)[1]	11	397–427	0.055–0.129	1.279	−1.279
Aucejo *et al.* (2006)[46]	12	316–377	0.003–0.03	1.285	1.285
		Saturated liquid density			
Neubeck (1887)[36]	11	364–416		0.724	−0.724
Perkin (1896)[47]	6	277–298		0.383	−0.383
Miller (1932)[48]	4	273–293		0.012	−0.012
Francis (1957)[49]	25	373–608		0.503	−0.212
Panchenkov *et al.* (1958)[50]	7	293–353		0.281	0.276
Hales and Townsend (1972)[51]	14	293–490		0.005	−0.003
Chirico *et al.* (1997)[22]	9	323–523		0.602	0.336
		Saturated vapor density			
Chirico *et al.* (1997)[22]	4	617–631		6.004	−2.903
		p-*ρ*-*T*			
Patterson (1902)[52]	5	292–309	0.101	6.929	6.887
Heil (1932)[53]	16	253–403	0.101	0.541	0.418
Massart (1936)[54]	10	250–428	0.101	0.097	0.064
Shraiber and Pechenyuk (1965)[55]	8	293–363	0.101	0.009	−0.009
Mamedov *et al.* (1967)[56]	59	298–548	0.1–40	0.041	0.009
Skinner *et al.* (1968)[57]	6	303	0.098–207	0.368	−0.324
Akhundov (1974)[58]	317	298–673	0.13–51	3.989	0.250
Hust and Schramm (1976)[59]	19	248–328	0.101	0.527	−0.466
Garg *et al.* (1993)[60]	72	318–373	0.1–10	0.048	−0.048
Jain *et al.* (1994)[61]	8	298–322	0.101	0.030	−0.030
Et-Tahir *et al.* (1995)[62]	45	298–363	0.1–40	0.198	−0.198
Swain *et al.* (1997)[63]	5	293–318	0.101	1.342	−1.342
Moumouzias *et al.* (1999)[64]	5	288–308	0.101	0.055	0.018
Moumouzias and Ritzoulis (2000)[65]	5	288–308	0.101	0.055	0.018
Swain *et al.* (2000)[66]	5	293–318	0.101	1.271	−1.271
Swain *et al.* (2001)[67]	9	293–318	0.101	1.440	−1.440
Wang *et al.* (2005)[68]	7	293–353	0.101	3.405	−3.390
Chen *et al.* (2007)[69]	8	293–353	0.101	0.039	−0.039
Yang *et al.* (2007)[70]	7	298–353	0.101	0.103	−0.103
Gonzalez-Olmos and Iglesias (2008)[71]	15	288–323	0.101	0.121	−0.121
Song *et al.* (2008)[72]	7	303–333	0.101	0.065	0.065
Nain *et al.* (2008)[73]	7	288–318	0.101	0.055	−0.055
		Sound speed			
Al-Kandary *et al.* (2006)[74]	4	288–303	0.101	0.225	0.225
Nain (2007)[75]	4	288–318	0.101	0.691	0.691
Nain (2007)[76]	4	288–318	0.101	0.691	0.691
Gonzalez-Olmos and Iglesias (2008)[71]	15	288–323	0.101	0.516	−0.516

TABLE 8. Summary of experimental data for *o*-xylene—Continued

Author	Number of points	Temperature range (K)	Pressure range (MPa)	AAD (%)	Bias (%)
Second virial coefficient[a]					
Andon *et al.* (1957)[77]	2	377–393		50.339	50.339
Cox and Andon (1958)[78]	3	409–438		64.982	64.982
Hossenlopp and Archer (1988)[79]	9	353–446		28.830	14.311
Heat of vaporization					
Hossenlopp and Archer (1988)[79]	9	353–446		0.076	0.076
Saturation heat capacity					
Huffman *et al.* (1930)[80]	8	253–295		0.846	−0.846
Pitzer and Scott (1943)[39]	15	250–302		0.257	0.242
Chirico *et al.* (1997)[22]	35	252–550		0.131	0.109
Isobaric heat capacity					
Williams and Daniels (1924)[81]	10	303–348	0.101	3.355	−3.355
Jain *et al.* (1992)[82]	7	304–322	0.101	0.142	0.142
Garg *et al.* (1993)[60]	36	318–373	0.1–10	0.515	−0.515

[a]For the second virial coefficient, the AAD stands for average absolute difference with the unit of $cm^3 \, mol^{-1}$, and the Bias stands for average difference with the unit of $cm^3 \, mol^{-1}$.

these data. This gave a slight offset to the data of Chirico *et al.*[22] but showed excellent agreement with the data of Hales and Townsend.[51] Above 500 K, the data of Francis[49] have higher uncertainties, as verified by other data sets at lower temperatures, and were not used in the fit of the equation. There is only one data set for saturated vapor density;[22] these near-critical data were not used in fitting the equation.

Comparisons of single-phase densities calculated with the equation of state to experimental data are shown in Fig. 4. The equation generally represents the data within 0.1% in

the compressed-liquid region, and up to 1.0% in the critical region, except for the data reported by Hust and Schramm[59] and Et-Tahir *et al.*[62] The equation represents the data of Mamedov *et al.*[56] with an AAD of 0.041%. The data of Garg *et al.*[60] are the most recent high-pressure data; these data show agreement of about 0.05% with the equation, and slightly higher differences with respect to other data. The data reported by Mamedov *et al.*[56] and Akhundov[58] agree with each other very well in the region where they overlap. At higher temperatures (above 560 K), the only other data published are those by Akhundov,[58] hence it is hard to

FIG. 2. Comparisons of vapor pressures calculated with the equation of state to experimental data for *o*-xylene.

+ Other data sets
□ Ambrose *et al.* (1967)
* Castellari *et al.* (1982)
⧓ Diaz Pena *et al.* (1979)
▷ Glaser and Ruland (1957)
⬆ Kassel (1936)
⊤ Neubeck (1887)
⊙ Pitzer and Scott (1943)
▲ Willingham *et al.* (1945)
× Ambrose (1987)
○ Aucejo *et al.* (2006)
◇ Chirico *et al.* (1997)
△ Forziati *et al.* (1949)
⅄ Hessler and Lichtenstein (1986)
↗ Mamedov *et al.* (1970)
⊟ Nigam and Mahl (1971)
◇ Rodrigues *et al.* (2005)
⊔ Woringer (1900)

FIG. 3. Comparisons of saturated liquid densities calculated with the equation of state to experimental data for *o*-xylene.

+ Other data sets
□ Francis (1957)
* Miller (1932)
⧓ Panchenkov *et al.* (1958)
× Chirico *et al.* (1997)
○ Hales and Townsend (1972)
◇ Neubeck (1887)
△ Perkin (1896)

FIG. 4. Comparisons of densities calculated with the equation of state to experimental data for *o*-xylene.
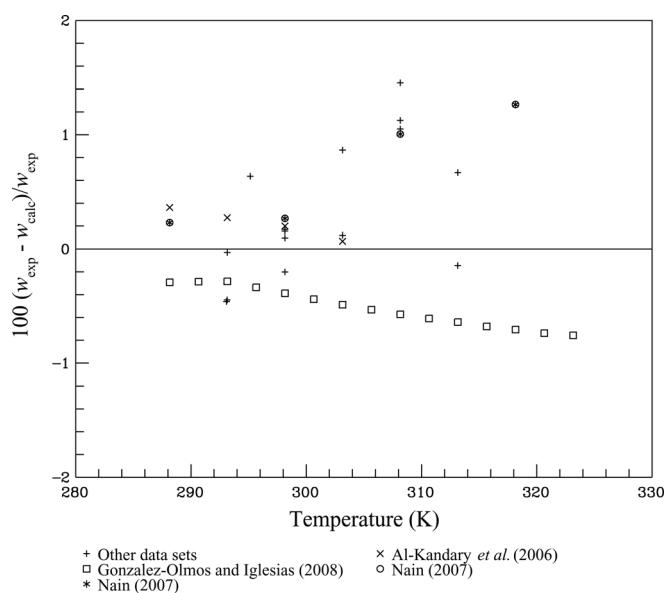
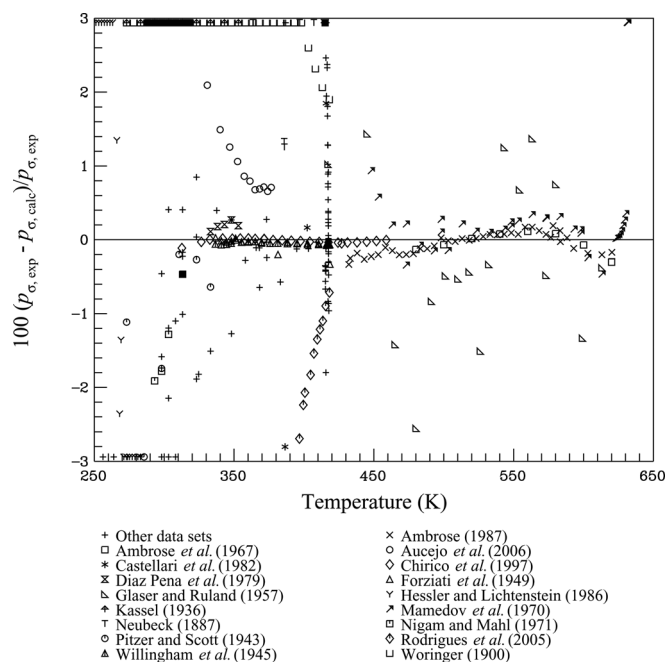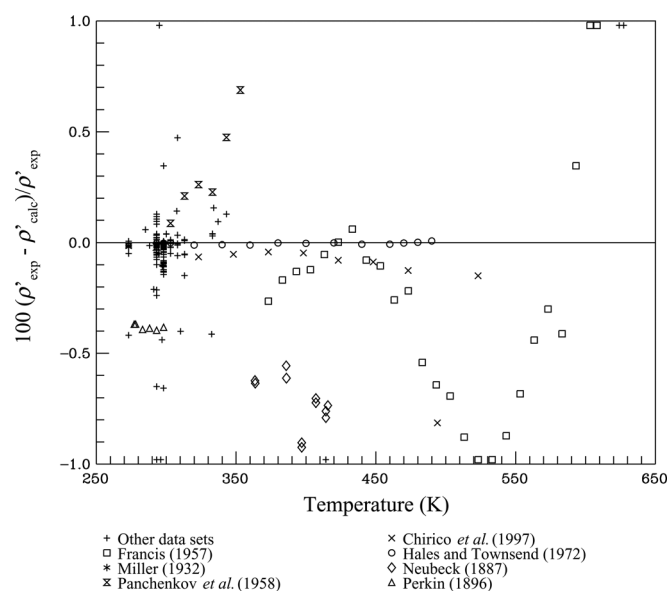FIG. 5. Comparisons of sound speeds calculated with the equation of state to experimental data for *o*-xylene.
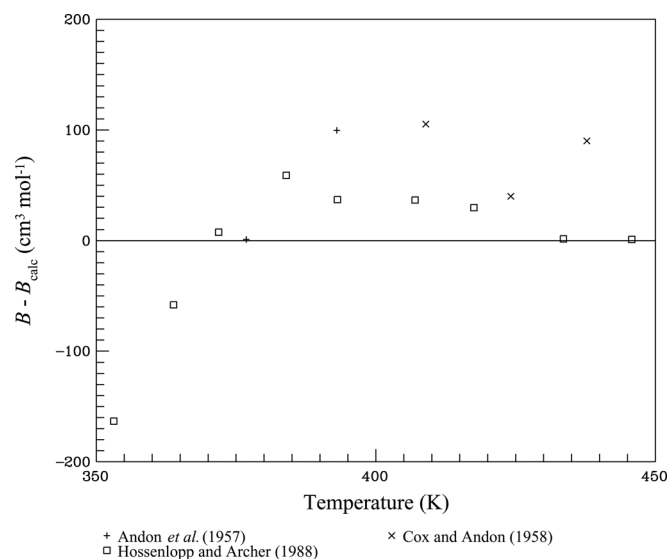
FIG. 6. Comparisons of second virial coefficients calculated with the equation of state to experimental data for *o*-xylene.

estimate the uncertainty of the equation of state and experimental data.

Figure 5 compares sound speeds calculated with the equation of state to experimental data; the equation represents these data generally within 0.5%. These data are available at atmospheric pressure only, and are very scattered, as shown in Fig. 5. The data of Gonzalez-Olmos and Iglesias[71] show negative deviations, while most of the other data show positive deviations. Comparisons of second virial coefficients calculated with the equation of state to experimental data are presented in Fig. 6; these data were not used in fitting. Figure 7, in which the y-intercept (zero density) represents the second virial coefficient at a given temperature, and where the third virial coefficient can be taken from the slope of each line at zero density, shows that the behavior of the

FIG. 7. Calculations of $(Z-1)/\rho$ along isotherms versus density for *o*-xylene.

FIG. 8. Comparisons of saturation heat capacities calculated with the equation of state to experimental data for *o*-xylene.
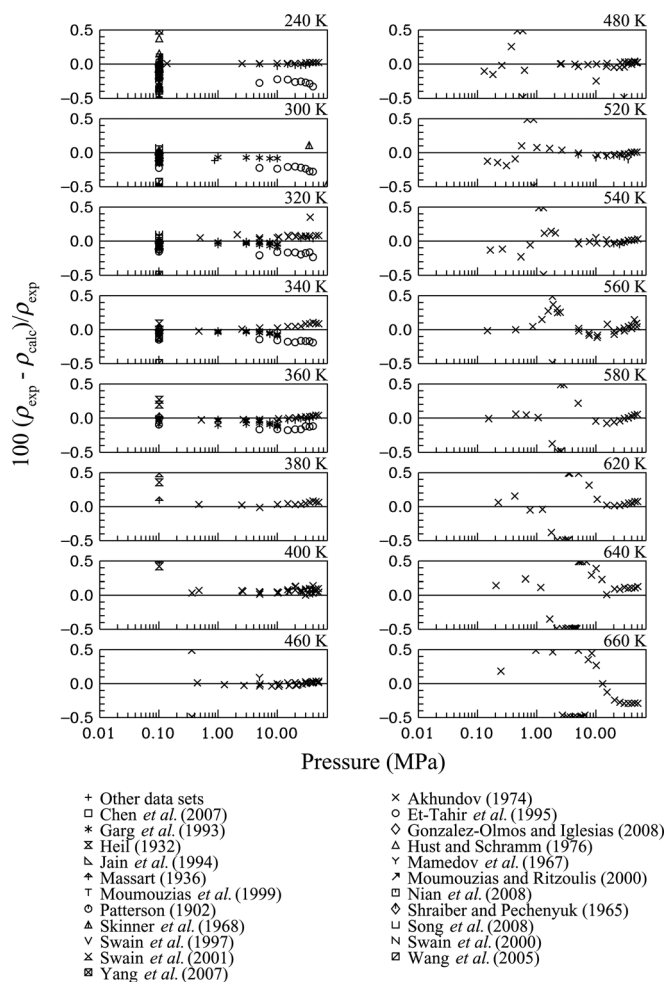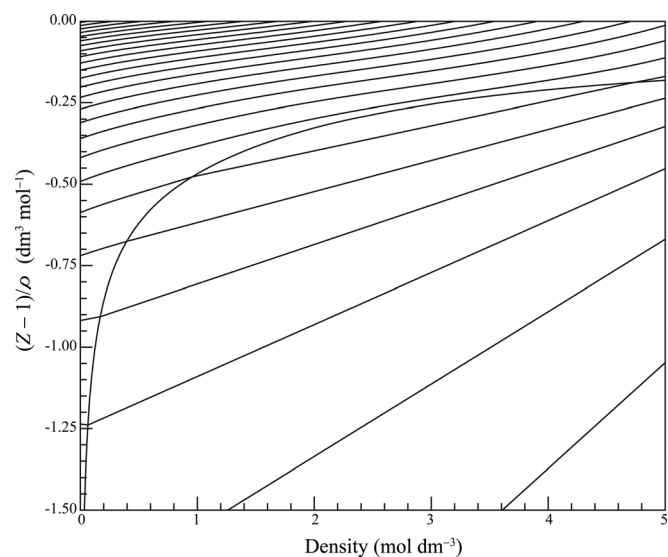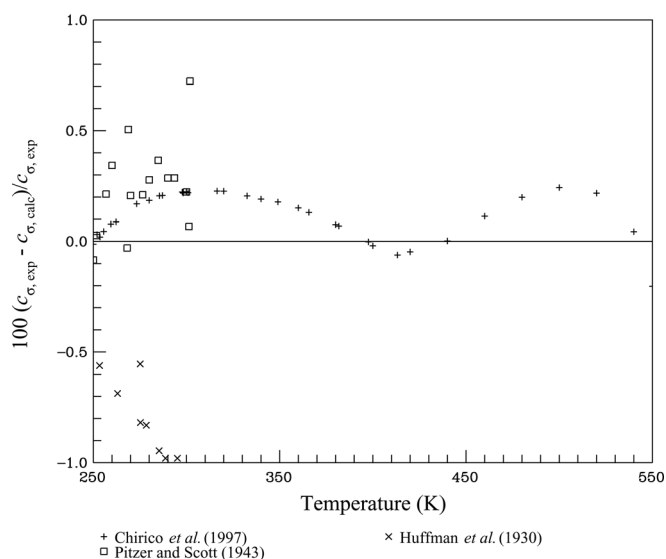
second and third virial coefficients as well as the shape of the equation of state are reasonable. This plot helps demonstrate that vapor-phase properties are consistent with those of other fluids that have reliable vapor-phase data.

Figure 8 compares saturation heat capacities calculated with the equation of state to experimental data; the equation represents the experimental data generally within 0.5%. The data of Huffman *et al.*[80] deviate substantially from the other two data sets. The equation agrees with recent data of Chirico *et al.*[22] to within 0.3%; the data extend over a large temperature range. Comparisons of calculated isobaric heat capacities are presented in Fig. 9. The equation represents the data generally within 1.0%. The data reported by Williams and Daniels[81] were measured nearly 90 years ago

+ Other data sets × Garg *et al.* (1993)
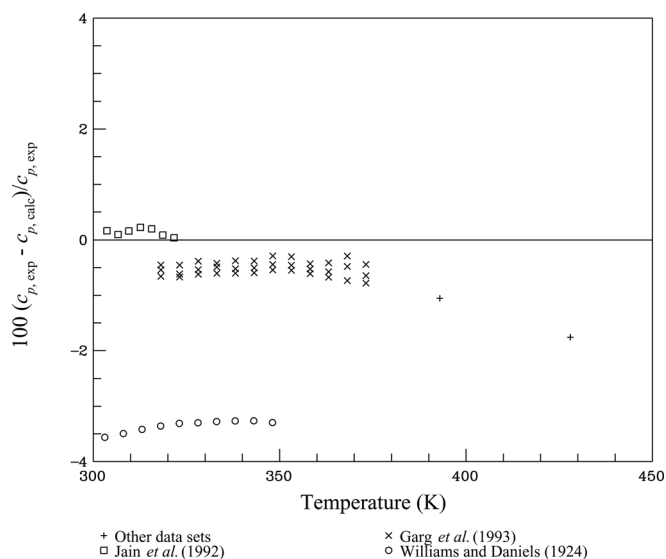□ Jain *et al.* (1992) ○ Williams and Daniels (1924)

FIG. 9. Comparisons of isobaric heat capacities calculated with the equation of state to experimental data for *o*-xylene.

and do not agree with the data of Garg *et al.*[60] The equation shows a +0.1% systematic deviation to the data of Jain *et al.*[82] at lower temperatures.

The uncertainty of the equation of state for *o*-xylene in vapor pressure is estimated to be 0.5% above 300 K. The uncertainty in saturated liquid density is 0.1% below 500 K, and increases to 0.5% at higher temperatures, due to a lack of experimental data. The uncertainties in density of the equation of state range from 0.1% in the compressed-liquid region to 1.0% in the critical and vapor regions. The uncertainty in sound speed is estimated to be 1.0%. The uncertainties in heat of vaporization, saturation heat capacity, and isobaric heat capacity are estimated to be 0.5%, 0.5%, and 1.0%, respectively. In the critical region, the uncertainties are higher for all properties.

2.2. Equation of state for *m*-xylene

Experimental data for *m*-xylene are summarized in Table 9. Figure 10 compares vapor pressures calculated with the equation of state to experimental data. Vapor pressures for *m*-xylene are scattered; the equation represents the consistent vapor pressures generally within 0.1% above 300 K. The data reported by Ambrose,[20] Ambrose *et al.*,[16] Chirico *et al.*,[85] Forziati *et al.*,[41] and Park and Gmehling[83] agree with each other. There are many data points at the normal boiling temperature, and the equation passes near the center of them. The data reported by Aucejo *et al.*,[46] Woringer,[37] Rodrigues *et al.*,[1] and Uno *et al.*[87] near the normal boiling temperature deviate substantially from this center, and appear to be unreliable. The data of Ambrose,[16,20] Chirico *et al.*,[85] and Forziati *et al.*[41] show very good agreement and formed the basis of the equation for vapor pressure. The Ambrose data are the only values above 450 K. These data scatter by as much as 0.5%, and the equation passes through the center. Below 320 K, the scatter in the data increases to about 1%, and these data were not used in the fit.

Comparisons of saturated liquid densities calculated with the equation of state to experimental data are shown in Fig. 11. The equation of state represents most of these data generally to within 0.1%. Some of the experimental saturated-liquid data for *m*-xylene are quite scattered, especially above 350 K. However, at the normal boiling point, there are many points that show very consistent behavior; the equation represents these data within 0.03%. The equation agrees most with the data of Chirico *et al.*[85] above 350 K. This trend is similar to that for the other fluids, and gives better confidence in the fit at the higher temperatures.

Figure 12 presents comparisons of single-phase densities calculated with the equation of state to experimental data; the equation represents the data of Chang and Lee,[92] Garg *et al.*,[60] Grigor'ev *et al.*,[91] and Caudwell[90] generally within 0.1%. The data of Chang *et al.*[93] show a +0.15% systematic deviation, and the data of Et-Tahir *et al.*[62] systematically deviate by −0.1%. Although there are no data below 290 K, the saturated liquid densities of Heil[53] down to 230 K show that the equation is still valid to lower temperatures, as is to

TABLE 9. Summary of experimental data for *m*-xylene

Author	Number of points	Temperature range (K)	Pressure range (MPa)	AAD (%)	Bias (%)
		Vapor pressure			
Neubeck (1887)[36]	9	362–412	0.02–0.102	2.309	−1.847
Woringer (1900)[37]	29	273–413	0–0.105	2.231	2.231
Kassel (1936)[38]	9	273–353	0–0.015	0.636	0.589
Pitzer and Scott (1943)[39]	6	273–333	0–0.007	0.810	0.516
Forziati *et al.* (1949)[41]	20	332–413	0.006–0.104	0.211	0.167
Glaser and Ruland (1957)[13]	17	412–606	0.101–3.04	3.612	−3.581
Ambrose *et al.* (1967)[16]	8	460–600	0.314–2.87	0.027	0.027
Diaz Peña *et al.* (1979)[43]	6	328–353	0.005–0.015	0.086	0.014
Ambrose (1987)[20]	47	428–617	0.152–3.52	0.080	−0.042
Park and Gmehling (1989)[83]	18	327–412	0.005–0.101	0.392	−0.213
Malanowski *et al.* (1994)[84]	8	361–410	0.02–0.096	0.101	−0.101
Chirico *et al.* (1997)[85]	24	309–453	0.002–0.27	0.020	−0.014
Rodrigues *et al.* (2005)[1]	18	362–423	0.022–0.137	0.994	0.948
Aucejo *et al.* (2006)[46]	15	308–372	0.002–0.03	1.158	1.158
Didaoui-Nemouchi *et al.* (2007)[86]	9	264–343	0–0.01	6.060	0.278
Uno *et al.* (2007)[87]	5	381–409	0.04–0.093	0.381	0.381
		Saturated liquid density			
Neubeck (1887)[36]	12	362–412		0.227	0.227
Perkin (1896)[47]	12	277–298		0.016	−0.010
Patterson (1902)[52]	5	293–315		0.026	−0.026
Tyrer (1914)[88]	10	273–372		0.042	0.036
Heil (1932)[53]	18	233–393		0.169	0.126
Azim *et al.* (1933)[89]	6	293–348		0.423	0.423
Massart (1936)[54]	7	273–399		0.114	0.091
Francis (1957)[49]	24	373–603		0.413	0.400
Shraiber and Pechenyuk (1965)[55]	16	293–363		0.012	0.003
Hales and Townsend (1972)[51]	14	293–490		0.104	0.104
Garg *et al.* (1993)[60]	12	318–373		0.022	−0.006
Jain *et al.* (1994)[61]	8	298–322		0.033	0.009
Et-Tahir *et al.* (1995)[62]	5	298–363		0.075	−0.074
Chirico *et al.* (1997)[85]	14	323–617		2.101	1.048
Moumouzias *et al.* (1999)[64]	5	288–308		0.036	0.024
Moumouzias and Ritzoulis (2000)[65]	5	288–308		0.035	0.019
Caudwell (2004)[90]	14	298–398		0.088	0.033
Wang *et al.* (2005)[68]	7	293–353		0.033	−0.011
Chen *et al.* (2007)[69]	8	293–353		0.008	0.001
Yang *et al.* (2007)[70]	7	298–353		0.025	0.025
		p-*ρ*-*T*			
Grigor'ev *et al.* (1983)[91]	5	573–673	0.1	0.024	0.007
Garg *et al.* (1993)[60]	60	318–373	1–10	0.045	−0.040
Chang and Lee (1995)[92]	39	298–348	1–20	0.030	−0.030
Et-Tahir *et al.* (1995)[62]	40	298–363	5–40	0.125	−0.125
Chang *et al.* (1996)[93]	18	333–413	5–30	0.148	0.148
Caudwell (2004)[90]	100	298–473	19.9–198	0.097	0.054
Nain *et al.* (2008)[73]	7	288–318	0.101	0.018	0.018
		Sound speed			
Aralaguppi *et al.* (1992)[94]	3	298–308	0.101	0.026	−0.016
Al-Kandary *et al.* (2006)[74]	4	288–303	0.101	0.462	−0.097
Nain (2007)[75]	4	288–318	0.101	0.182	0.092
Nain (2007)[76]	4	288–318	0.101	0.182	0.092
		Second virial coefficient[a]			
Andon *et al.* (1957)[77]	2	377–393		290.220	−290.220
Cox and Andon (1958)[78]	3	409–438		62.256	−62.256
Grigor'ev *et al.* (1983)[91]	5	573–673		11.464	−0.651

TABLE 9. Summary of experimental data for *m*-xylene—Continued

Author	Number of points	Temperature range (K)	Pressure range (MPa)	AAD (%)	Bias (%)
		Saturation heat capacity			
Huffman *et al.* (1930)[80]	6	217–275		0.568	0.568
Pitzer and Scott (1943)[39]	20	230–320		0.849	0.849
Chirico *et al.* (1997)[85]	36	225–550		0.081	−0.001
Paramo *et al.* (2003)[95]	14	288–348		0.205	0.203
Paramo *et al.* (2006)[96]	8	332–401		0.396	0.341
		Heat of vaporization			
Mathews (1926)[97]	1	411		0.541	0.541
Osborne and Ginnings (1947)[98]	1	298		0.108	−0.108
Cox and Andon (1958)[78]	1	412		0.079	−0.079
Anthoney *et al.* (1976)[99]	1	298		0.113	0.113
		Isobaric heat capacity			
San Jose *et al.* (1976)[100]	7	523–540	1–2.5	0.538	−0.538
Jain *et al.* (1992)[82]	7	304–322	0.101	0.258	−0.258
Garg *et al.* (1993)[60]	36	318–373	0.1–10	0.291	−0.283

[a]For the second virial coefficient, the AAD stands for average absolute difference with the unit of $cm^3\ mol^{-1}$, and the Bias stands for average difference with the unit of $cm^3\ mol^{-1}$.

be expected due to the good extrapolation behavior of the equation. There are only five data points above 473 K. Values for the second virial coefficients are very limited, and deviations are not given in a figure; however, the behavior of the second and third virial coefficients, as well as the shape of the equation of state, are reasonable, and a plot similar to Fig. 7 for *o*-xylene shows correct behavior. Comparisons of sound speeds calculated with the equation of state to experimental data are not presented in a figure, but the equation represents the saturated liquid sound-speed data, which are available only over a very limited temperature range, generally within 0.5%.

Figure 13 compares saturation heat capacities calculated with the equation of state to experimental data; the equation represents the data generally within 1.0%. The data of Paramo *et al.*[95,96] show an upward trend. The equation represents the data reported by Chirico *et al.*[85] within 0.15%

+ Other data sets
□ Ambrose (1987)
✳ Chirico *et al.* (1997)
⧖ Didaoui-Nemouchi *et al.* (2007)
◁ Glaser and Ruland (1957)
✦ Malanowski *et al.* (1994)
⊤ Park and Gmehling (1989)
⊙ Rodrigues *et al.* (2005)
▲ Woringer (1900)

× Ambrose *et al.* (1967)
○ Aucejo *et al.* (2006)
◇ Diaz Pena *et al.* (1979)
△ Forziati *et al.* (1949)
Y Kassel (1936)
↗ Neubeck (1887)
⊡ Pitzer and Scott (1943)
◇ Uno *et al.* (2007)

FIG. 10. Comparisons of vapor pressures calculated with the equation of state to experimental data for *m*-xylene.

+ Other data sets
□ Caudwell (2004)
✳ Chirico *et al.* (1997)
⧖ Francis (1957)
△ Hales and Townsend (1972)
✦ Jain *et al.* (1994)
⊤ Moumouzias *et al.* (1999)
⊙ Neubeck (1887)
△ Perkin (1896)
∨ Tyrer (1914)
× Yang *et al.* (2007)

× Azim *et al.* (1933)
○ Chen *et al.* (2007)
◇ Et-Tahir *et al.* (1995)
△ Garg *et al.* (1993)
Y Heil (1932)
↗ Massart (1936)
⊡ Moumouzias and Ritzoulis (2000)
◇ Patterson (1902)
⊔ Shraiber and Pechenyuk (1965)
Ͷ Wang *et al.* (2005)

FIG. 11. Comparisons of saturated liquid densities calculated with the equation of state to experimental data for *m*-xylene.

FIG. 12. Comparisons of densities calculated with the equation of state to experimental data for *m*-xylene.

below 520 K, and there is a downward trend at higher temperatures (above 500 K). The data of Pitzer and Scott[39] and two of the Huffman et al.[80] data points are consistent with each other, but not with other data. These data were not used in the fit. Calculated isobaric heat capacities are compared in
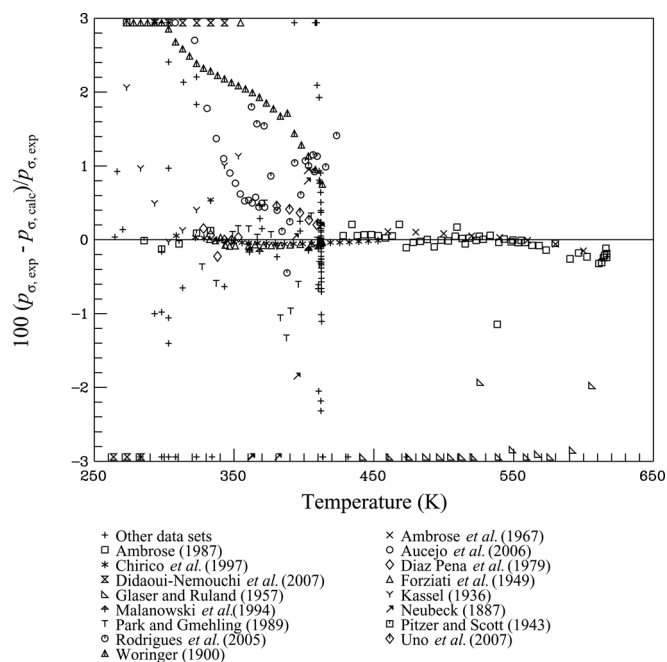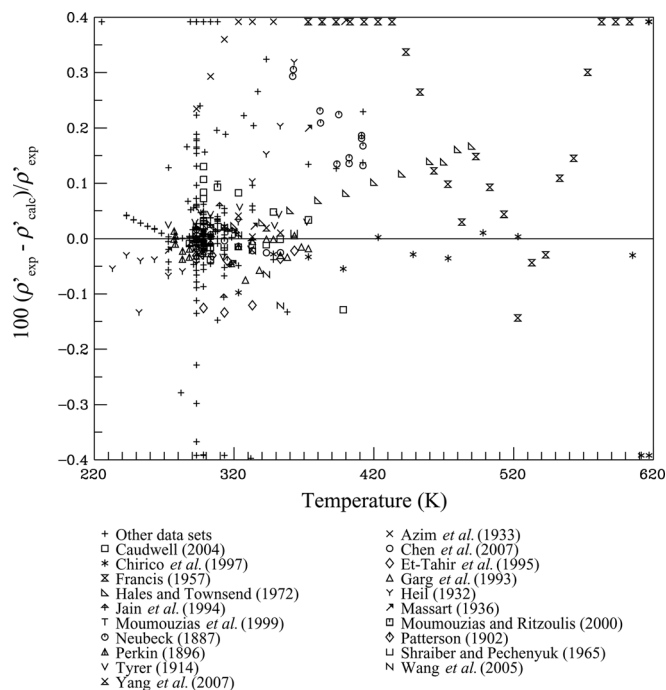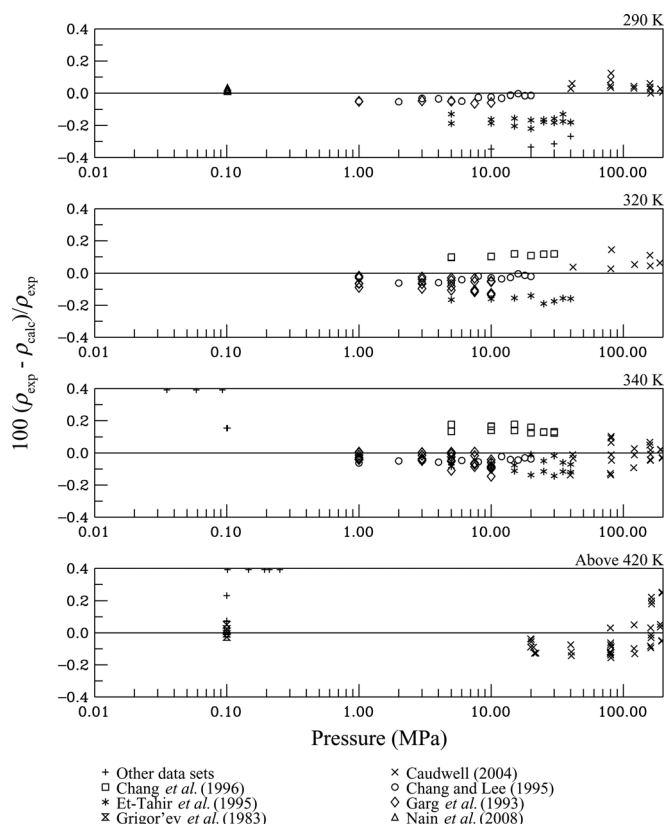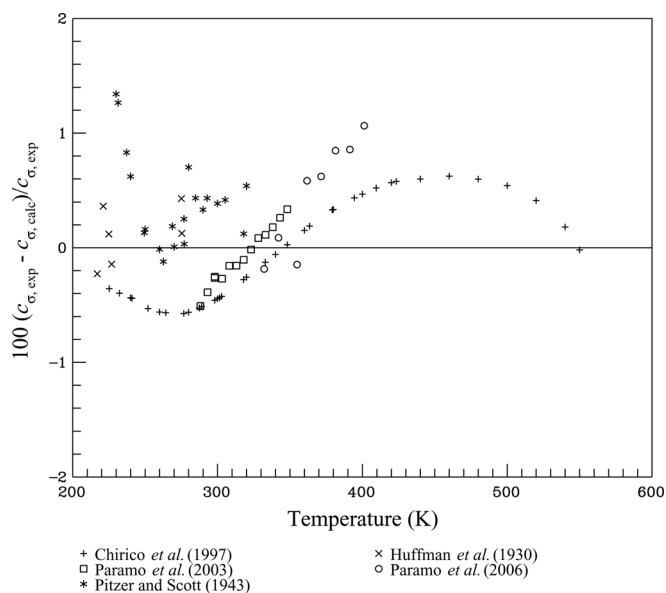

FIG. 13. Comparisons of saturation heat capacities calculated with the equation of state to experimental data for *m*-xylene.
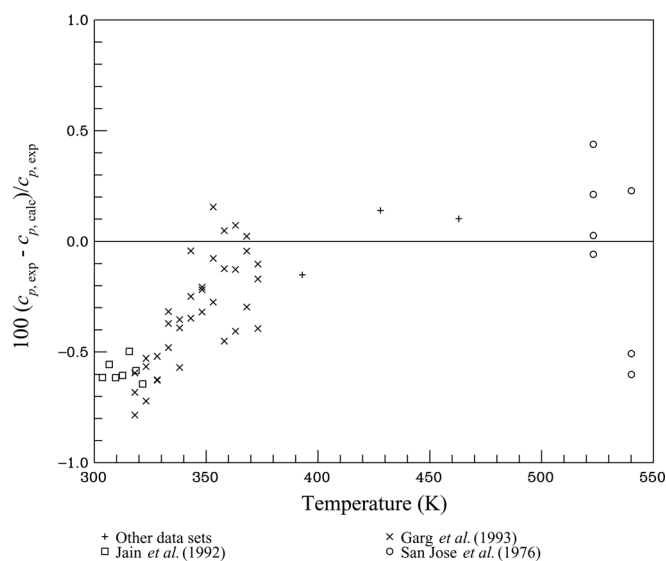

FIG. 14. Comparisons of isobaric heat capacities calculated with the equation of state to experimental data for *m*-xylene.

Fig. 14. The equation represents the data within 0.5%. Because isobaric heat capacities and saturation heat capacities are nearly the same at low temperatures, the close representation of the equation with the data of Chirico et al.[85] means that the isobaric heat-capacity data of Jain et al.[82] and Garg et al.[60] deviate from the Chirico et al. data on average by about 0.3%.

The uncertainty of the equation of state for *m*-xylene in vapor pressure is 0.2% above 300 K. The uncertainty in saturated liquid density is 0.1% between 230 K and 400 K, and increases to 0.2% at higher and lower temperatures, due to a lack of experimental data. The uncertainty in density is 0.2% in the compressed-liquid region, and 1.0% elsewhere, including the critical and vapor regions. The uncertainty in sound speed in the liquid phase is estimated to be 0.5%. The uncertainty in saturation and isobaric heat capacity is 0.5%.

2.3. Equation of state for *p*-xylene

Table 10 summarizes the experimental data for *p*-xylene and the AADs between experimental data and values calculated with the equation of state. Comparisons of vapor pressures calculated with the equation of state to experimental data are presented in Fig. 15. The equation represents vapor pressures generally within 0.5%. The data of Willingham et al.,[40] Forziati et al.,[41] Chianese and Marrelli,[102] and Diaz Peña et al.[43] agree with each other from 330 K to the normal boiling temperature. The equation represents these data to within 0.05%. The data reported by Mamedov et al.,[19] Ambrose et al.,[16] and Ambrose[20] agree with each other below 580 K, and show opposite deviations near the critical point (above 600 K). The data of Woringer[37] and Aucejo et al.,[46] which deviate from most of the other data sets, appear to have higher uncertainties. Below 300 K, the scatter in the data increases rapidly, and there are no data points

TABLE 10. Summary of experimental data for *p*-xylene

Author	Number of points	Temperature range (K)	Pressure range (MPa)	AAD (%)	Bias (%)
Vapor pressure					
Neubeck (1887)[36]	10	360–412	0.02–0.101	0.856	−0.385
Woringer (1900)[37]	29	273–413	0.001–0.106	29.133	29.133
Kassel (1936)[38]	9	273–353	0–0.015	7.968	−7.968
Willingham *et al.* (1945)[40]	20	331–412	0.006–0.104	0.021	−0.020
Forziati *et al.* (1949)[41]	18	332–412	0.006–0.104	0.042	−0.003
Glaser and Ruland (1957)[13]	17	411–608	0.101–3.04	3.788	−3.682
Ambrose *et al.* (1967)[16]	8	460–600	0.317–2.88	0.072	−0.054
Mamedov *et al.* (1970)[19]	37	448–616	0.245–3.62	0.466	0.391
Nigam and Mahl (1971)[42]	6	293–303	0.001	0.782	−0.570
Osborn and Douslin (1974)[101]	21	341–452	0.01–0.27	0.060	−0.026
Diaz Peña *et al.* (1979)[43]	6	328–353	0.005–0.016	0.077	0.069
Castellari *et al.* (1982)[44]	6	380–410	0.04–0.099	0.502	0.090
Chianese and Marrelli (1985)[102]	11	393–443	0.061–0.221	0.184	0.184
Natarajan and Viswanath (1985)[103]	14	411–557	0.102–1.62	2.045	−0.050
Ambrose (1987)[20]	47	428–614	0.155–3.43	0.130	−0.084
Smith (1990)[104]	7	293–323	0.001–0.004	0.806	−0.587
Llopis and Monton (1994)[105]	8	367–378	0.025–0.037	0.707	−0.707
Rodrigues *et al.* (2005)[1]	9	390–421	0.053–0.13	1.507	−1.496
Aucejo *et al.* (2006)[46]	15	307–371	0.002–0.03	1.373	1.373
Saturated liquid density					
Neubeck (1887)[36]	11	360–412		0.066	−0.028
Block (1912)[106]	10	285–308		0.054	−0.019
Jaeger (1917)[107]	6	299–399		0.062	0.041
Richards *et al.* (1924)[108]	6	273–334		0.083	0.069
Timmermans and Martin (1926)[109]	9	288–306		0.004	−0.003
Heil (1932)[53]	12	293–403		0.055	0.024
Fairbrother (1934)[110]	6	293–393		0.043	0.040
Massart (1936)[54]	8	288–399		0.029	0.026
Francis (1957)[49]	21	423–613		0.775	0.112
Panchenkov *et al.* (1958)[50]	7	293–353		0.101	0.093
Shraiber and Pechenyuk (1965)[55]	8	293–363		0.006	0.001
Hales and Townsend (1972)[51]	14	293–490		0.014	−0.004
Akhundov (1974)[58]	40	298–618		0.413	0.349
Qin *et al.* (1992)[111]	7	293		0.024	0.024
Tasioula-Margari and Demetropoulos (1992)[112]	5	298–318		0.011	−0.003
Garg *et al.* (1993)[60]	12	318–373		0.034	−0.029
Jain *et al.* (1994)[61]	8	298–322		0.026	−0.025
Exarchos *et al.* (1995)[113]	5	293–313		0.025	−0.025
Konti *et al.* (1997)[114]	5	288–308		0.019	−0.012
Avraam *et al.* (1998)[115]	5	288–308		0.016	−0.007
Resa *et al.* (2004)[116]	5	293–313		0.023	−0.023
Yang *et al.* (2004)[117]	7	298–353		0.007	0.004
Wang *et al.* (2005)[68]	7	293–353		0.033	0.031
Di *et al.* (2006)[118]	9	298–353		0.027	0.020
Chen *et al.* (2007)[69]	7	293–353		0.091	0.064
Yang *et al.* (2007)[70]	7	298–353		0.007	0.007
Gonzalez-Olmos and Iglesias (2008)[71]	15	288–323		0.001	0.000
Song *et al.* (2008)[72]	7	303–333		0.049	−0.049
p-ρ-*T*					
Akhundov (1974)[58]	283	323–673	0.155–50.7	0.309	0.007
Bich *et al.* (1981)[119]	16	423–563	0.1	0.077	−0.077
Hossenlopp and Scott (1981)[120]	7	348–439	0.013–0.1	0.058	0.043
Yokoyama *et al.* (1990)[121]	40	283–298	10–200	0.203	0.203
Garg *et al.* (1993)[60]	60	318–373	1–10	0.057	−0.056
Et-Tahir *et al.* (1995)[62]	32	313–363	5–40	0.083	−0.079
Nain *et al.* (2008)[73]	7	288–318	0.101	0.010	−0.125

TABLE 10. Summary of experimental data for *p*-xylene—Continued

Author	Number of points	Temperature range (K)	Pressure range (MPa)	AAD (%)	Bias (%)
Sound speed					
Resa *et al.* (2004)[116]	5	293–313	Sat. liq.	0.077	0.049
Al-Kandary *et al.* (2006)[74]	4	288–303	Sat. liq.	0.186	0.186
Nain (2007)[75]	4	288–318	Sat. liq.	0.370	0.370
Nain (2007)[76]	4	288–318	Sat. liq.	0.370	0.370
Gonzalez-Olmos and Iglesias (2008)[71]	15	288–323	Sat. liq.	0.142	−0.084
Second virial coefficient[a]					
Andon *et al.* (1957)[77]	2	377–393		52.689	−52.689
Cox and Andon (1958)[78]	3	409–438		37.176	34.134
Bich *et al.* (1981)[119]	16	423–563		31.847	31.847
Hossenlopp and Scott (1981)[120]	7	348–439		43.248	−18.124
Heat of vaporization					
Hossenlopp and Scott (1981)[120]	7	348–439		0.061	−0.061
Natarajan and Viswanath (1985)[103]	14	411–557		1.125	1.125
Saturation heat capacity					
Huffman *et al.* (1930)[80]	5	291–299		1.078	−1.078
Pitzer and Scott (1943)[39]	15	290–360		1.193	1.105
Corruccini and Ginnings (1947)[122]	16	286–573		0.423	−0.422
Messerly *et al.* (1988)[123]	24	286–390		0.076	0.063
Chirico *et al.* (1997)[22]	10	380–550		0.528	0.303
Isobaric heat capacity					
Williams and Daniels (1924)[81]	10	303–348	0.101	3.318	−3.318
Ott *et al.* (1979)[124]	9	288–328	0.101	0.282	−0.217
Hossenlopp and Scott (1981)[120]	24	398–523	0.013–0.203	0.211	0.211
Jain *et al.* (1992)[82]	7	304–322	0.101	0.276	−0.276
Garg *et al.* (1993)[60]	36	318–373	0.1–10	0.536	−0.536

[a]For the second virial coefficient, the AAD stands for average absolute difference with the unit of $cm^3 \, mol^{-1}$, and the Bias stands for average difference with the unit of $cm^3 \, mol^{-1}$.

+ Other data sets
□ Ambrose *et al.* (1967)
* Castellari *et al.* (1982)
⌧ Diaz Pena *et al.* (1979)
⌐ Glaser and Ruland (1957)
♠ Llopis and Monton (1994)
T Natarajan and Viswanath (1985)
⊙ Nigam and Mahl (1971)
△ Rodrigues *et al.* (2005)
∨ Willingham *et al.* (1945)

× Ambrose (1987)
○ Aucejo *et al.* (2006)
◇ Chianese and Marrelli (1985)
△ Forziati *et al.* (1949)
Y Kassel (1936)
↗ Mamedov *et al.* (1970)
⊡ Neubeck (1887)
◇ Osborn and Douslin (1974)
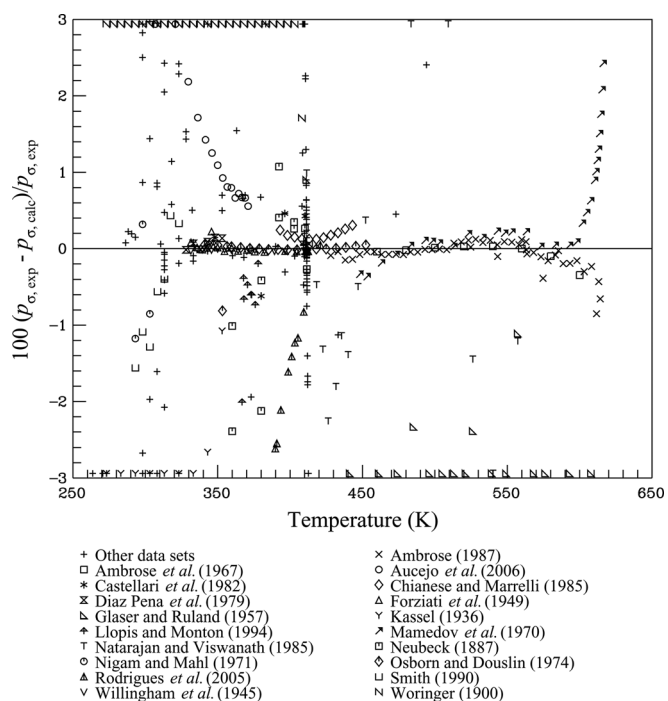⊔ Smith (1990)
N Woringer (1900)

FIG. 15. Comparisons of vapor pressures calculated with the equation of state to experimental data for *p*-xylene.

with low enough uncertainties to which the equation could be fitted.

Figure 16 compares saturated liquid densities calculated with the equation of state to experimental data; the equation represents saturated liquid densities generally within 0.05% below 380 K. At higher temperatures, the data of Hales and Townsend[51] help validate the equation of state. The data reported by Francis[49] and Akhundov[58] are less reliable; the Francis data are quite scattered and do not help with the assessment of the uncertainty in the equation, even though they extend to the critical point. There is some agreement among the data of Hales and Townsend and of Akhundov, and the equation represents most of these data to within 0.05%.

Figure 17 compares densities calculated with the equation of state to experimental data. The equation represents densities generally within 0.2% in the liquid region, and 1.0% elsewhere, including the critical and vapor regions. The equation represents the data reported by Akhundov[58] generally within 0.1%, except those in the critical region. The data of Garg *et al.*[60] and Et-Tahir *et al.*[62] agree with the data of Akhundov,[58] although they cover a much smaller temperature range. The data reported by Yokoyama *et al.*[121] extend to high pressures; they deviate from the data of Garg *et al.*[60]
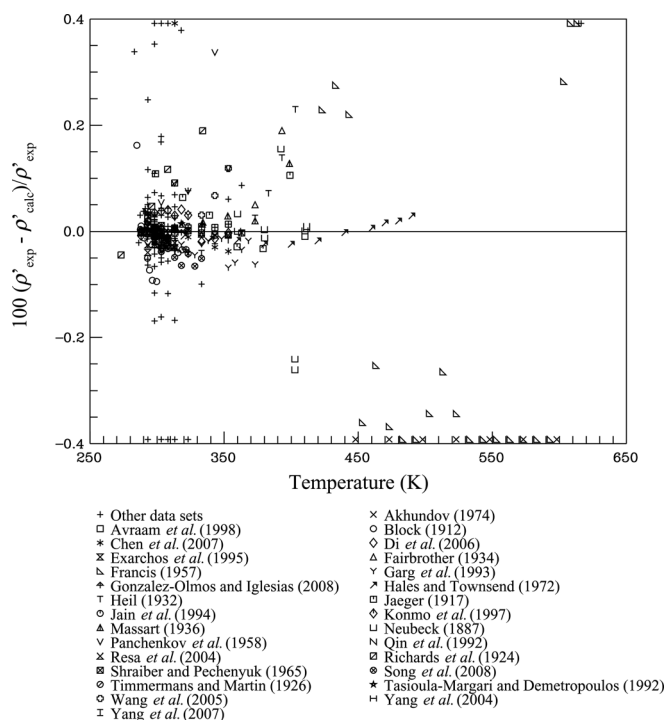
FIG. 16. Comparisons of saturated liquid densities calculated with the equation of state to experimental data for *p*-xylene.
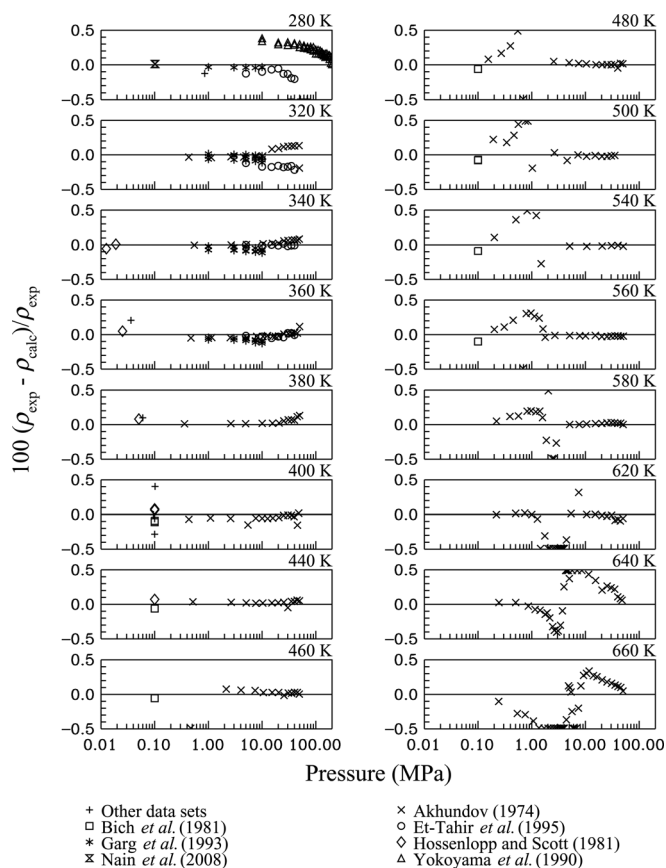

FIG. 17. Comparisons of densities calculated with the equation of state to experimental data for *p*-xylene.

and Et-Tahir *et al.*[62] at low pressures by 0.4%. The equation represents the data of Yokoyama *et al.* at high pressures, even though the data were not used in fitting. The virial coefficients are very limited, and not displayed in this work; the equation represents second virial coefficients generally within 50 cm^3 mol^{-1}; however, the behavior of the second and third virial coefficients, as well as the shape of the equation of state, are reasonable, and a plot similar to Fig. 7 shows correct behavior. Saturated liquid sound speeds calculated with the equation of state are compared to experimental data in Fig. 18; the equation represents the data within 1.0%. Many of the data are scattered within 0.3% of the equation. The data of Gonzalez-Olmos and Iglesias[71] show deviations of as much as −0.3%; these data cover the largest temperature range, from 288 K to 323 K. All the other data sets show positive deviations.

The equation shows good comparisons (to within 0.1%) with the heat of vaporization data of Hossenlopp and Scott,[120] but the data of Natarajan and Viswanath[103] deviate by more than 1%. Because the enthalpies of vaporization and the slope of the vapor pressure curve are closely linked through the Clausius–Clapeyron equation, the uncertainties in the data of Hossenlopp and Scott should be much lower than those of the data of Natarajan and Viswanath. Figure 19 gives comparisons of saturation heat capacities calculated with the equation of state to experimental data; the equation represents the data generally within 1.0%. The data reported by Chirico *et al.*[22] and Messerly *et al.*[123] agree with each other very well, and the equation represents the data generally within 0.5%, except those approaching the critical point. The data of Huffman *et al.*[80] and Pitzer and Scott[39] show large scatter, with one set above the equation and the other below. The data of Corruccini and Ginnings[122] show a trend different from the data of Chirico *et al.* at high temperatures, and it is unclear which data set should be preferred in fitting.
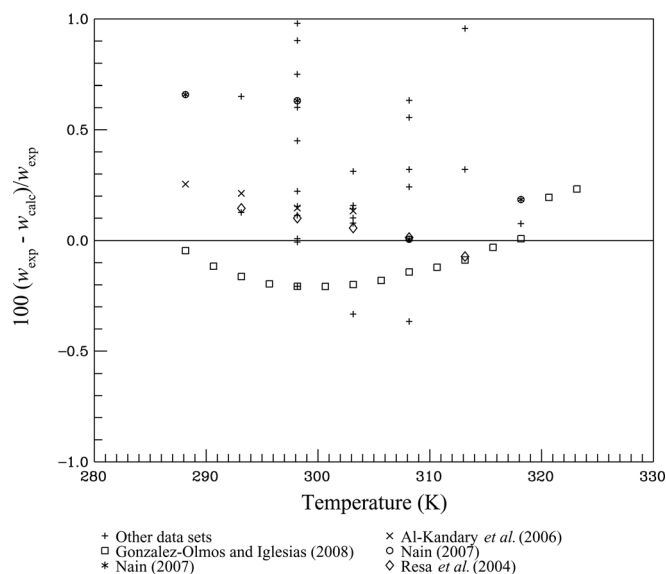

FIG. 18. Comparisons of saturated sound speeds calculated with the equation of state to experimental data for *p*-xylene.
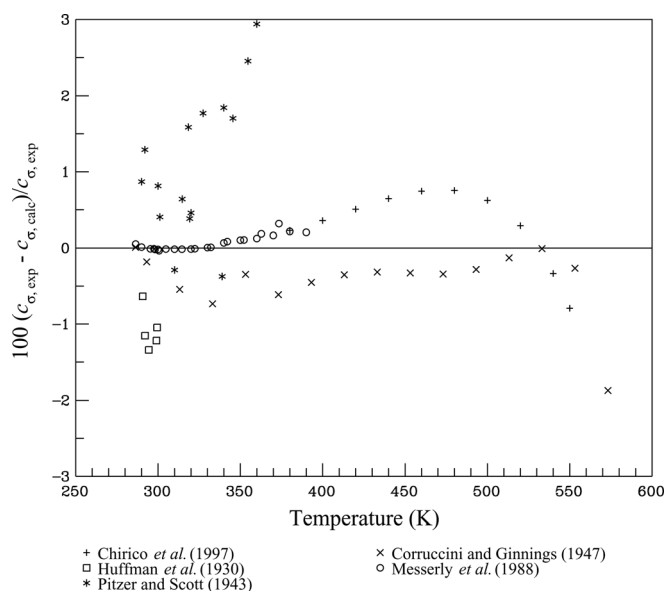
FIG. 19. Comparisons of saturation heat capacities calculated with the equation of state to experimental data for *p*-xylene.

FIG. 20. Comparisons of isobaric heat capacities calculated with the equation of state to experimental data for *p*-xylene.

Figure 20 compares heat capacities calculated with the equation of state to experimental data; the equation represents these values generally within 0.7%, except for the data of Williams and Daniels,[81] which are not reliable.

The uncertainty in vapor pressure of the equation of state for *p*-xylene is 0.2% above 300 K. The uncertainties in saturated liquid density are 0.02% between 290 K and 350 K, and 0.2% elsewhere, due to a lack of reliable experimental data. The uncertainties in density are 0.2% in the liquid
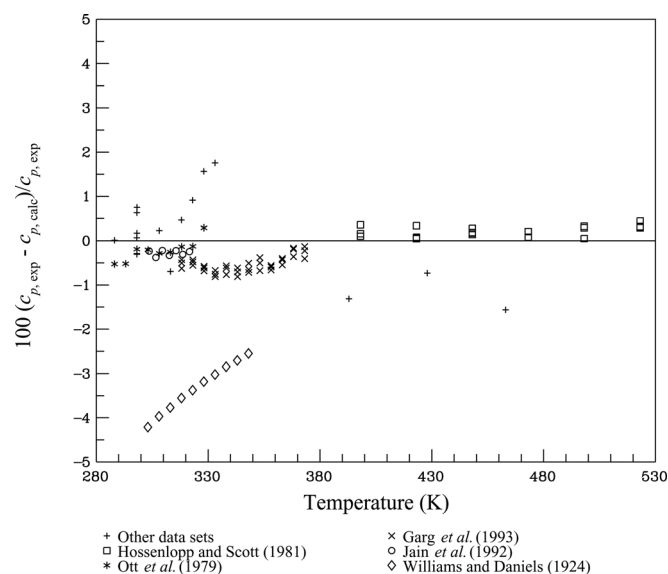
region and 1.0% elsewhere, including the critical and vapor regions. The uncertainty in sound speed is 0.3% in the liquid region, and the uncertainty in heat capacity is 1.0%.

2.4. Equation of state for ethylbenzene

Experimental data available for ethylbenzene are summarized in Table 11. Comparisons of vapor pressures calculated with the equation of state to experimental data are shown in Fig. 21; the equation represents many of the measurements

TABLE 11. Summary of experimental data for ethylbenzene

Author	Number of points	Temperature range (K)	Pressure range (MPa)	AAD (%)	Bias (%)
		Vapor pressure			
Woringer (1900)[37]	28	273–408	0.001–0.104	30.718	30.718
Scott and Brickwedde (1945)[125]	16	273–297	2.58×10^{-4}–9.05×10^{-4}	0.815	−0.815
Willingham et al. (1945)[40]	20	330–410	0.006–0.104	0.020	0.009
Buck et al. (1949)[126]	13	336–409	0.008–0.101	1.423	1.003
Forziati et al. (1949)[41]	20	330–410	0.006–0.104	0.049	0.042
Dreyer et al. (1955)[127]	9	301–409	0.002–0.101	6.036	2.512
Yang and Van Winkle (1955)[128]	8	331–410	0.007–0.101	0.335	−0.335
Chaiyavech (1959)[129]	5	299–366	0.001–0.027	0.222	−0.184
Ambrose et al. (1967)[16]	8	460–600	0.333–2.92	0.129	0.063
Kraus and Linek (1971)[130]	14	350–405	0.015–0.099	0.739	0.680
Funk et al. (1972)[131]	5	313–353	0.003–0.017	0.141	−0.096
Akhundov (1973)[132]	36	448–620	0.259–3.72	0.454	0.377
Jain and Yadav (1974)[133]	12	303–323	0.002–0.005	4.952	4.952
Akhundov et al. (1976)[134]	32	298–620	0.001–3.72	0.365	0.308
Osborn and Scott (1980)[135]	21	339–450	0.01–0.27	0.039	0.039
Chianese and Marrelli (1985)[102]	11	393–443	0.065–0.234	0.840	0.840
Ambrose (1987)[20]	42	424–615	0.148–3.53	0.151	0.023
Malanowski et al. (1994)[84]	8	358–407	0.02–0.096	0.045	−0.040
Chirico et al. (1997)[29]	23	306–450	0.002–0.27	0.035	0.033
Von Niederhausern et al. (2000)[30]	9	493–617	0.618–3.62	0.731	−0.731
Zhao and Kabadi (2004)[136]	5	498–613	0.681–3.45	0.451	0.451

TABLE 11. Summary of experimental data for ethylbenzene—Continued

Author	Number of points	Temperature range (K)	Pressure range (MPa)	AAD (%)	Bias (%)
Rodrigues et al. (2005)[1]	12	386–417	0.05–0.124	1.322	−1.283
Aucejo et al. (2006)[46]	15	305–369	0.002–0.03	1.151	1.151
Uno et al. (2007)[87]	5	378–406	0.04–0.093	0.706	0.706
Matsuda et al. (2010)[137]	6	378–408	0.04–0.099	0.111	−0.083
		Saturated liquid density			
Landolt and Jahn (1892)[138]	4	288–293		0.343	0.343
Perkin (1896)[47]	12	277–298		0.126	0.125
Azim et al. (1933)[89]	7	293–348		0.483	0.483
Massart (1936)[54]	12	178–399		0.043	−0.012
Vogel (1948)[139]	4	293–359		0.153	0.153
Griffel et al. (1954)[140]	4	300–303		0.043	0.043
Panchenkov and Erchenkov (1962)[141]	6	283–353		0.073	0.067
Hales and Townsend (1972)[51]	14	293–490		0.093	−0.089
Akhundov (1974)[58]	40	473–598		0.295	0.275
Akhundov et al. (1976)[134]	32	298–620		0.335	0.312
Singh et al. (1989)[142]	5	298–333		1.242	1.242
Chylinski and Gregorowicz (1991)[143]	5	298–333		0.014	−0.007
Francesconi and Comelli (1991)[144]	10	292–305		0.010	0.010
Qin et al. (1992)[111]	6	293		0.083	0.083
Garg et al. (1993)[60]	12	318–373		0.065	−0.065
Jain et al. (1995)[145]	4	298–322		0.019	0.007
Chirico et al. (1997)[29]	6	610–617		5.285	−5.285
George and Sastry (2003)[146]	4	298–313		0.025	0.025
Resa et al. (2004)[116]	5	293–313		0.031	0.031
Yang et al. (2004)[147]	5	298–333		0.214	0.214
Naziev et al. (2005)[148]	4	292–359		0.025	−0.010
Gonzalez-Olmos et al. (2007)[149]	15	288–323		0.020	−0.010
Song et al. (2008)[72]	7	303–333		0.015	−0.007
		Saturated vapor density			
Akhundov et al. (1976)[134]	32	298–620		1.984	1.867
		p-ρ-T			
Hossenlopp and Scott (1981)[120]	9	473–673	0.01–0.1	0.034	0.026
Chylinski and Gregorowicz (1991)[143]	18	318–333	0.401–5.03	0.026	−0.026
Garg et al. (1993)[60]	60	318–373	1–10	0.094	−0.093
Naziev et al. (2005)[148]	62	292–490	5–58.9	0.179	0.175
		Sound speed			
Korabel'nikov (1971)[150]	45	193–633	Sat. liq.	2.374	−1.223
Resa et al. (2004)[116]	6	293–313	Sat. liq.	0.073	0.073
Gonzalez-Olmos et al. (2007)[149]	19	288–323	Sat. liq.	0.088	0.015
		Second virial coefficient[a]			
Hossenlopp and Scott (1981)[120]	9	346–437		21.254	−18.638
		Heat of vaporization			
Hossenlopp and Scott (1981)[120]	9	346–437		0.052	−0.048
Svoboda et al. (1982)[151]	3	328–358		0.384	−0.384
		Saturation heat capacity			
Huffman et al. (1930)[80]	21	178–550		1.005	−1.005
Blacet et al. (1931)[152]	16	185–305		2.844	1.854
Smith and Andrews (1931)[153]	25	286–368		1.959	−1.959
Kolossowsky and Udovenko (1934)[154]	9	184–298		4.545	−4.545
Scott and Brickwedde (1945)[125]	27	178–300		0.215	0.200
Chirico et al. (1997)[29]	40	178–550		0.155	0.092
Paramo et al. (2003)[95]	14	288–348		0.239	0.237
Paramo et al. (2006)[96]	7	332–391		0.622	0.622

TABLE 11. Summary of experimental data for ethylbenzene—Continued

Author	Number of points	Temperature range (K)	Pressure range (MPa)	AAD (%)	Bias (%)
		Isobaric heat capacity			
Williams and Daniels (1924)[81]	9	303–343	0.101	2.502	−2.502
Guthrie et al. (1944)[155]	29	180–305	0.101	0.160	0.142
Akhundov and Sultanov (1975)[156]	339	302–693	4–25	0.571	0.093
Mamedov et al. (1976)[157]	98	481–693	0.5–3.5	3.518	2.136
Andolenko and Grigor'ev (1979)[158]	10	293–393	0.101	0.494	−0.274
Hossenlopp and Scott (1981)[120]	28	386–523	0.013–0.203	0.137	0.042
Jain et al. (1992)[82]	7	304–322	0.101	0.485	0.485
Garg et al. (1993)[60]	36	318–373	0.1–10	0.360	−0.340

[a]For the second virial coefficient, the AAD stands for average absolute difference with the unit of $cm^3 \, mol^{-1}$, and the Bias stands for average difference with the unit of $cm^3 \, mol^{-1}$.

of the vapor pressure generally within 0.8% (with the highest deviations in the data of Akhundov et al.[134]). The data reported by Scott and Brickwedde,[125] Rodrigues et al.,[1] Aucejo et al.,[46] Buck et al.,[126] and Chianese and Marrelli[102] are all in good agreement, and the equation of state shows deviations of up to 0.1%. The data reported by Akhundov,[132] Zhao and Kabadi,[136] and Willingham et al.[40] deviate from the data reported by Ambrose[20] and Ambrose et al.[16] by about 0.4%–0.6%. The data of Ambrose appear to be more consistent with other vapor-pressure measurements at lower temperatures, and fit better with other data types.

In Fig. 22, saturated liquid densities calculated with the equation of state and experimental data are compared. The equation represents saturated liquid densities generally

within 0.05% between 290 K and 330 K. At higher temperatures, the data reported by Hales and Townsend[51] and Akhundov et al.[132,134] show opposite trends, with differences from the equation of state of −0.2% and +0.2%, respectively. Additional measurements in this region are needed to clarify this situation. There is only one set for the saturated vapor density available for ethylbenzene reported by Akhundov et al.;[134] the data were not used in fitting. The equation represents the data within 1.0% below 470 K. The experimental density data for ethylbenzene are very limited and scattered, as shown in Fig. 23. The equation represents the data of Hossenlopp and Scott[120] and Chylinski and Gregorowicz[143] within 0.1%, and the data of Garg et al.[60] and Naziev et al.[148] within 0.3%. There is only one set of experimental second virial coefficients. The equation represents the data
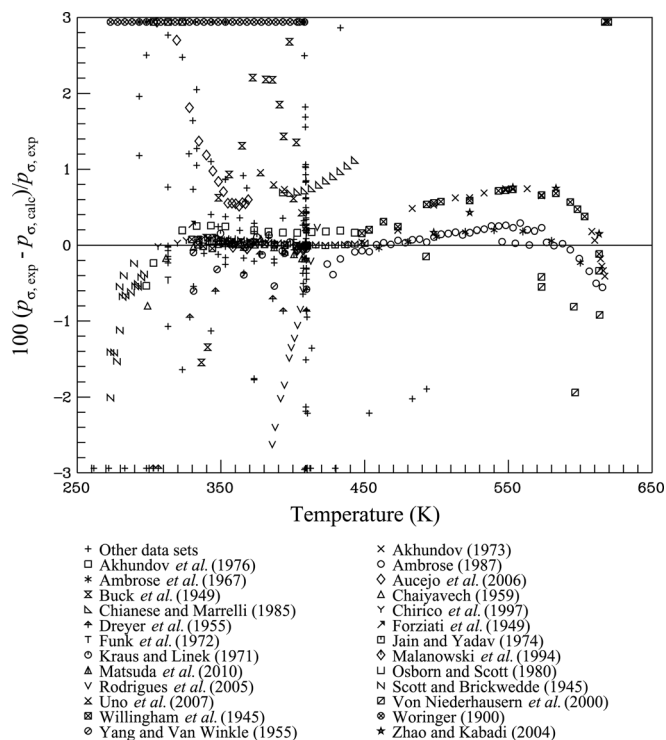

+ Other data sets
□ Akhundov et al. (1976)
∗ Ambrose et al. (1967)
⊠ Buck et al. (1949)
◹ Chianese and Marrelli (1985)
⊹ Dreyer et al. (1955)
⊤ Funk et al. (1972)
⊘ Kraus and Linek (1971)
▲ Matsuda et al. (2010)
∨ Rodrigues et al. (2005)
⋈ Uno et al. (2007)
⊠ Willingham et al. (1945)
⊘ Yang and Van Winkle (1955)

× Akhundov (1973)
○ Ambrose (1987)
◇ Aucejo et al. (2006)
△ Chaiyavech (1959)
◺ Chirico et al. (1997)
↗ Forziati et al. (1949)
⊞ Jain and Yadav (1974)
◇ Malanowski et al. (1994)
⊡ Osborn and Scott (1980)
N Scott and Brickwedde (1945)
⊘ Von Niederhausern et al. (2000)
⊗ Woringer (1900)
★ Zhao and Kabadi (2004)

FIG. 21. Comparisons of vapor pressures calculated with the equation of state to experimental data for ethylbenzene.

+ Other data sets
□ Akhundov et al. (1976)
∗ Chirico et al. (1997)
⊠ Francesconi and Comelli (1991)
◹ George and Sastr (2003)
⊹ Griffel et al. (1954)
⊤ Jain et al. (1995)
⊙ Massart (1936)
▲ Panchenkov and Erchenkov (1962)
∨ Qin et al. (1992)
⋈ Singh et al. (1989)
⊠ Vogel (1948)

× Akhundov (1973)
⊠ Azim et al. (1933)
◇ Chylinski and Gregorowicz (1991)
△ Garg et al. (1993)
Y Gonzalez-Olmos et al. (2007)
↗ Hales and Townsend (1972)
⊔ Landolt and Jahn (1892)
◇ Naziev et al. (2005)
⊔ Perkin (1896)
N Resa et al. (2004)
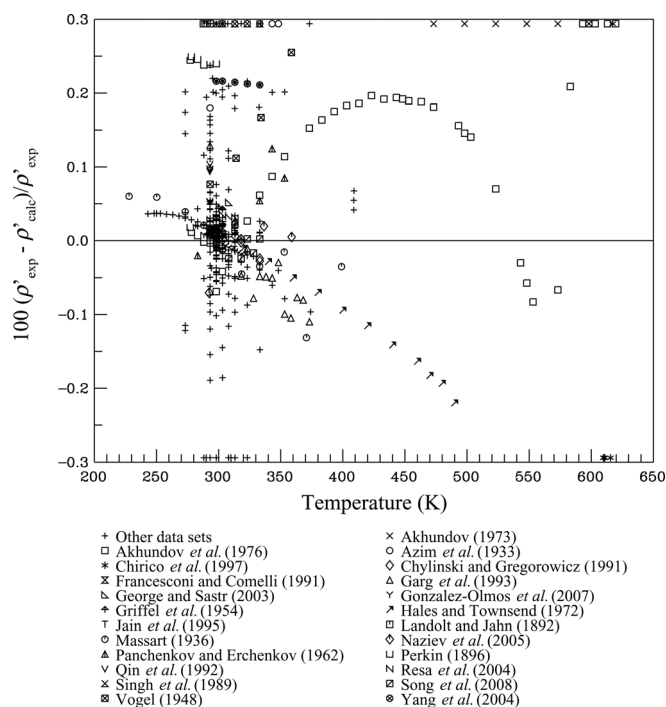⊡ Song et al. (2008)
⊗ Yang et al. (2004)

FIG. 22. Comparisons of saturated liquid densities calculated with the equation of state to experimental data for ethylbenzene.
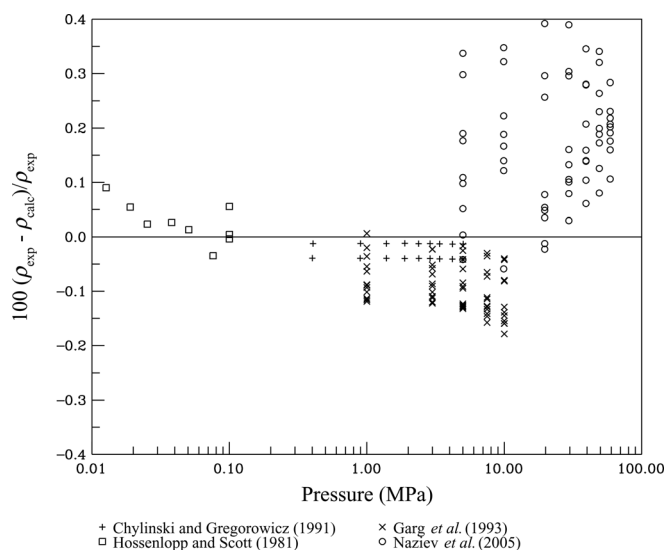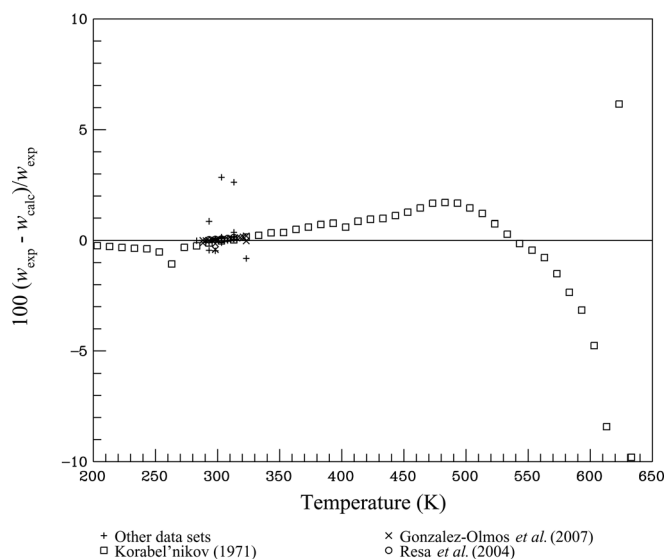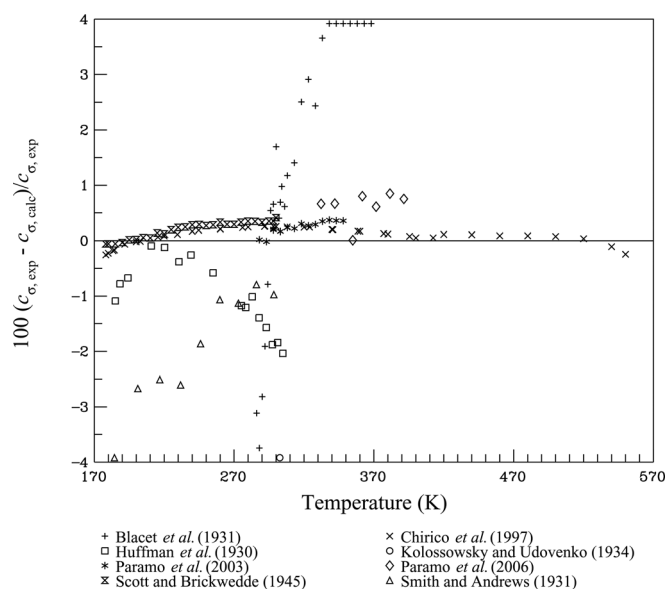
FIG. 23. Comparisons of densities calculated with the equation of state to experimental data for ethylbenzene.

generally within 25 cm^3 mol^{-1}; however, the behavior of the second and third virial coefficients as well as the shape of the equation of state are reasonable, and a plot similar to Fig. 7 for *o*-xylene shows correct behavior.

Saturated liquid sound speeds calculated with the equation of state are compared with experimental data in Fig. 24. Korabel'nikov[150] measured liquid-phase values from 193 K to 633 K. Below 400 K, the equation agrees with these data to within 1%, and between 400 K and 560 K, the deviations increase up to 2%.

Saturation heat capacities calculated with the equation of state are compared in Fig. 25; the equation deviates from the data of Scott and Brickwedde,[125] Paramo *et al.*,[95] and Chirico *et al.*[29] by up to 0.4%. The data of Blacet *et al.*,[152] Huff-

FIG. 25. Comparisons of saturation heat capacities calculated with the equation of state to experimental data for ethylbenzene.

man *et al.*,[80] and Smith and Andrews[153] show substantially higher deviations. All of these data cover a very wide temperature range from 170 K to 550 K, which helped the fitting of the equation in the absence of other wide-ranging data. This is further substantiated by the isobaric heat-capacity data shown in Fig. 26. The equation represents the data within 0.7% below 550 K (as shown by the deviations in the data of Guthrie *et al.*,[155] Garg *et al.*,[60] Andolenko and Grigor'ev,[158] Akhundov and Sultanov,[156] Hossenlopp and Scott,[120] and Mamedov *et al.*[157]), and within 1.5% at higher temperatures. The data reported by Williams and Daniels[81]

FIG. 24. Comparisons of saturated liquid sound speeds calculated with the equation of state to experimental data for ethylbenzene.
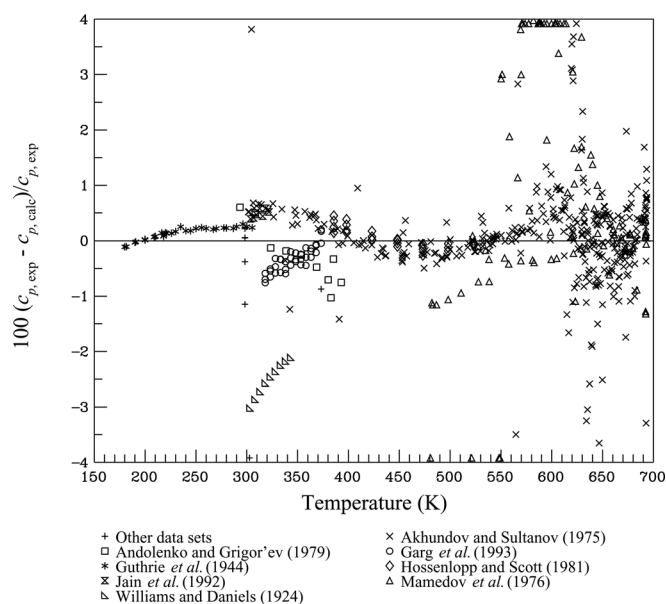

FIG. 26. Comparisons of isobaric heat capacities calculated with the equation of state to experimental data for ethylbenzene.

are less reliable. These isobaric heat-capacity data extend to 700 K, some of which are in the critical region.

The uncertainty of the equation of state for ethylbenzene in vapor pressure is 0.3%. The uncertainties in saturated liquid density are 0.1% below 350 K and 0.2% at higher temperatures. The uncertainties in density are 0.1% below 5 MPa, 0.2% at higher pressures in the liquid region, and 1.0% in the critical and vapor regions. The uncertainties in saturation and isobaric heat capacities and in the speed of sound are estimated to be 1.0%.

3. Extrapolation

The equations of state developed here have reasonable extrapolation behavior. Plots of constant property lines on various thermodynamic coordinates are useful in assessing how well the equations of state extrapolate. As the plots of these four fluids are all similar, not all are given here. The equations of state developed in this work were used to plot temperature versus isochoric heat capacity (Fig. 27), isobaric heat capacity (Fig. 28), density (Fig. 29), sound speed (Fig. 30), Gruneisen coefficient (Fig. 31), and pressure versus density (Fig. 32), as well as characteristic curves of the equation of state (Fig. 33).

Figures 27 and 28 show that the heat capacity increases as temperature decreases in the liquid region at low temperatures; this is quite common among fluids and has been validated experimentally for many fluids.[5] Figure 29 shows that the rectilinear diameter is straight at higher temperatures, as it should be, clear up to the critical point. Figure 30 shows that the saturated sound speed line for the liquid remains straight down to about 10 K, a reduced temperature of 0.016, and Fig. 32 indicates that the extrapolation behavior of the density at high temperatures and pressures is correct. This smooth behavior comes from the term $t_i = 1$, corresponding to the largest d_i of the polynomial terms ($d_i = 5$ for o-xylene,

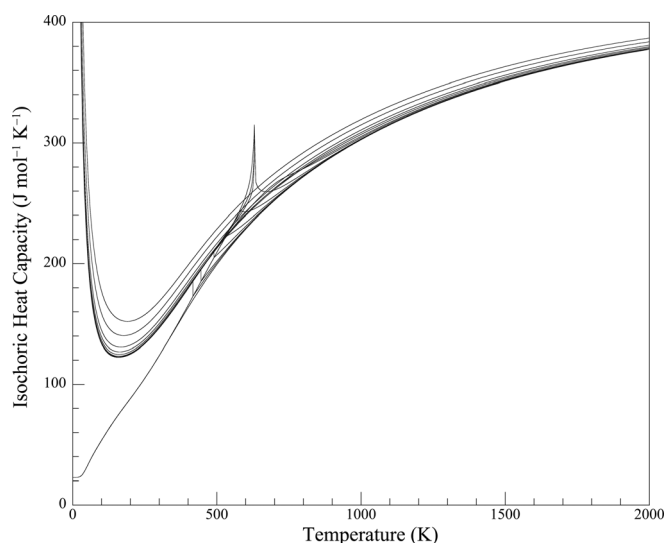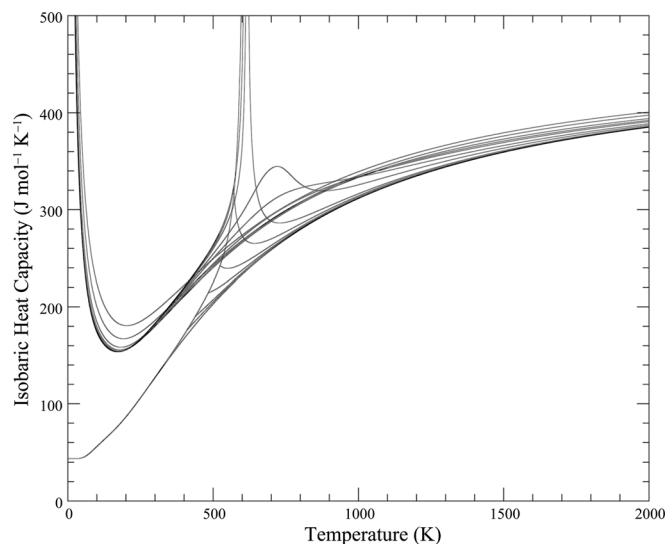
FIG. 28. Isobaric heat capacity versus temperature diagram plotted with the equation of state of p-xylene. Isobars are shown at pressures of (0, 0.1, 0.2, 0.5, 1, 2, p_c, 10, 20, 50, 100, 200, 500, and 1000) MPa.

p-xylene, and ethylbenzene; $d_i = 8$ for m-xylene), as explained by Lemmon and Jacobsen.[159]

The Gruneisen coefficient γ, which cannot be measured directly, is given by

$$\gamma = v \left(\frac{\partial p}{\partial e} \right)_v = \frac{\alpha_v k_s}{c_p \rho} = \frac{\alpha_v k_T}{c_v \rho}. \tag{10}$$

The Gruneisen coefficient is a combination of different properties, and the reasonable behavior of the Gruneisen coefficient, shown in Fig. 31, indicates that other properties and the equation of state are more likely to be correct because of the sensitive nature of this property.[160]
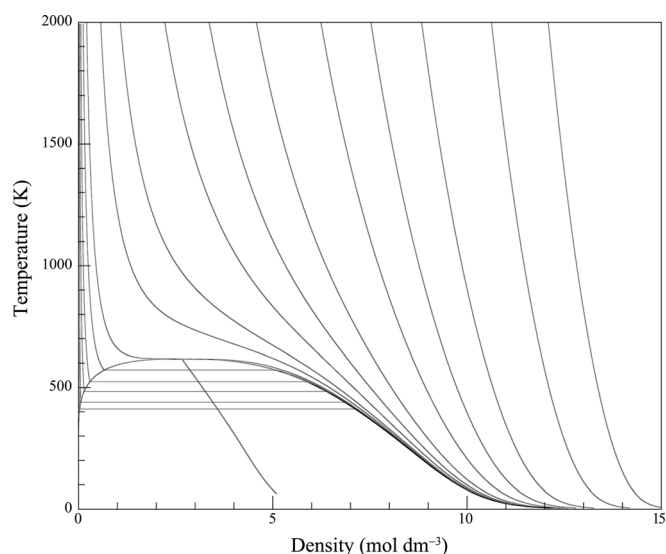

FIG. 27. Isochoric heat capacity versus temperature diagram plotted with the equation of state of o-xylene. Isobars are shown at pressures of (0, 0.1, 0.2, 0.5, 1, 2, p_c, 10, 20, 50, 100, 200, 500, and 1000) MPa.

FIG. 29. Temperature versus density diagram plotted with the equation of state of m-xylene. The straight line intersecting the critical point is the rectilinear diameter. Isobars are shown at pressures of (0.1, 0.2, 0.5, 1, 2, p_c, 10, 20, 50, 100, 200, 500, 1000, 2000, 5000, and 10000) MPa.
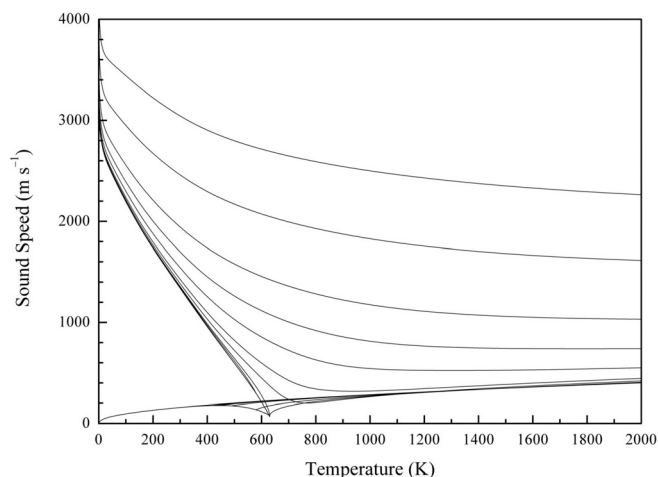
FIG. 30. Sound speed versus temperature diagram plotted with the equation of state of *o*-xylene. Isobars are shown at pressures of (0, 0.1, 0.2, 0.5, 1, 2, p_c, 10, 20, 50, 100, 200, 500, and 1000) MPa.

Plots of certain characteristic curves as shown in Fig. 33 are useful in assessing the behavior of an equation of state in regions far away from the available data.[5,7,35] The characteristic curves include the Boyle curve, the Joule–Thomson inversion curve, the Joule inversion curve, and the ideal curve. The Boyle curve is given by

$$\left(\frac{\partial Z}{\partial v}\right)_T = 0. \tag{11}$$

The Joule-Thomson inversion curve is given by

$$\left(\frac{\partial Z}{\partial T}\right)_p = 0. \tag{12}$$

FIG. 32. Pressure versus density diagram plotted with the equation of state of *p*-xylene. The straight line intersecting the critical point is the rectilinear diameter. Isotherms are shown at temperatures of (T_{tp}, 350, 400, 450, 500, 550, T_c, 10^3, 10^4, 10^5, 10^6, 10^7, 10^8, 10^9, and 10^{10}) K.

The Joule inversion curve is given by

$$\left(\frac{\partial Z}{\partial T}\right)_v = 0. \tag{13}$$

The ideal curve is given by

$$Z \equiv \frac{p}{\rho RT} = 1. \tag{14}$$

Overall, these plots indicate that the behavior of the equations of state developed here is appropriate within the range of validity, and that the extrapolation behavior is reasonable outside these ranges.
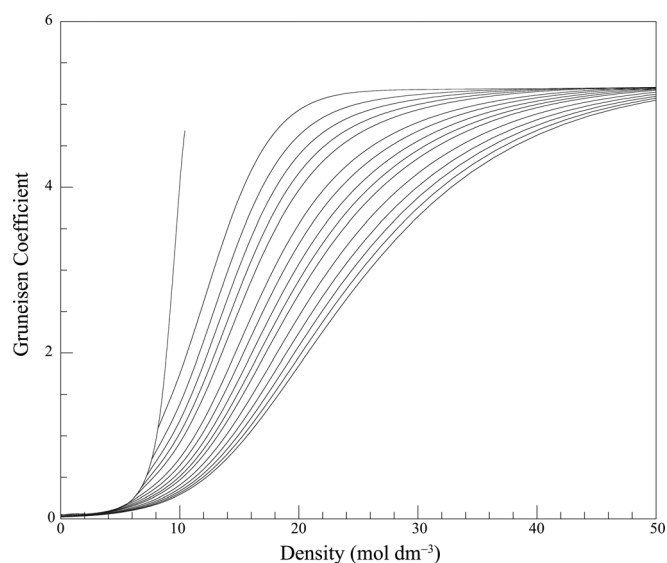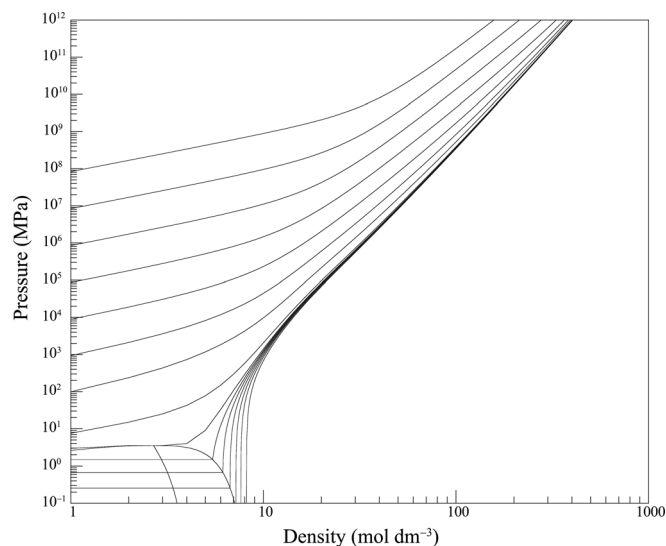

FIG. 31. Gruneisen coefficient versus density diagram plotted with the equation of state of *p*-xylene. Isotherms are shown at temperatures of (T_{tp}, 350, 400, 450, 500, T_c, 700, 800, 900, 1000, 1200, 1400, 1600, 1800, and 2000) K.
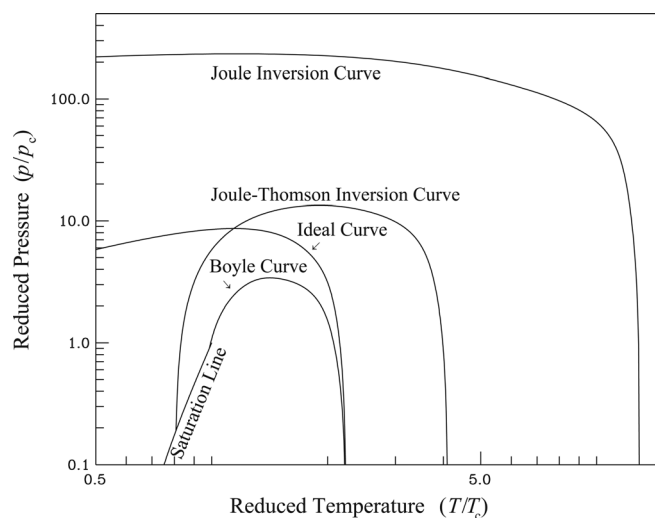

FIG. 33. Characteristic curves of the equation of state as a function of reduced temperature and reduced pressure plotted with the equation of state of ethylbenzene.

4. Conclusions

In this work, equations of state for the xylene isomers (*o*-xylene, *m*-xylene, and *p*-xylene) and ethylbenzene have been developed with the Helmholtz energy as the fundamental property, with independent variables of density and temperature. Overall, the uncertainties ($k = 2$, indicating a level of confidence of 95%) of the equations of state are 0.5% in vapor pressure at temperatures a little below the normal boiling point to those near the critical point. (Each fluid has slightly different values based on the comparisons to the data.) The uncertainties increase at lower temperatures due to a lack of experimental data. The uncertainties in density range from 0.02% in several cases for the saturated liquid density, to 0.1% in the liquid region, and then to 1.0% elsewhere, including the critical and vapor regions. The uncertainties in the properties related to energy (such as heat capacity and sound speed) are generally 1.0%. In the critical region, the uncertainties are higher for all properties. More detailed values are given in each section for the four fluids. As analyzed in the paper, the equations of state represent the experimental data accurately, and short functional forms have been used to achieve good behavior within the region of validity as well as at higher and lower temperatures and at higher pressures and densities.

There is a need for further measurement of the thermodynamic properties of xylene isomers and ethylbenzene, especially vapor pressure, saturated liquid density away from the normal boiling point, and caloric properties, including sound speed and heat capacity, in order to develop more accurate formulations for use in engineering system design and analysis.

5. References

[1] W. L. Rodrigues, S. Mattedi, and J. C. N. Abreu, J. Chem. Eng. Data **50**, 1134 (2005).

[2] S. Guo, M. S. Thesis, Tongji University, 2008.

[3] V. A. Welch, K. J. Fallon, and H.-P. Gelbke, in *Ullmann's Encyclopedia of Industrial Chemistry* (Wiley-VCH Verlag GmbH & Co. KGaA, 2000).

[4] W. L. Rodrigues, S. Mattedi, and J. C. N. Abreu, Braz. J. Chem. Eng. **22**, 453 (2005).

[5] E. W. Lemmon, M. O. McLinden, and W. Wagner, J. Chem. Eng. Data **54**, 3141 (2009).

[6] W. Wagner and A. Pruß, J. Phys. Chem. Ref. Data **31**, 387 (2002).

[7] R. Span, *Multiparameter Equations of State: An Accurate Source of Thermodynamic Property Data* (Springer, Berlin, 2000).

[8] M. Altschul, Z. Phys. Chem., Stoechiom. Verwandschaftsl. **11**, 577 (1893).

[9] J. C. Brown, J. Chem. Soc. Trans. **89**, 311 (1906).

[10] R. Fischer and T. Reichel, Mikrochem. Ver. Mikrochim. Acta **31**, 102 (1943).

[11] D. Ambrose and D. G. Grant, Trans. Faraday Soc. **53**, 771 (1957).

[12] A. W. Francis, Ind. Eng. Chem. **49**, 1787 (1957).

[13] F. Glaser and H. Ruland, Chem.-Ing.-Tech. **29**, 772 (1957).

[14] M. Simon, Bull. Soc. Chim. Belg. **66**, 375 (1957).

[15] M. J. Richardson and J. S. Rowlinson, Trans. Faraday Soc. **55**, 1333 (1959).

[16] D. Ambrose, B. E. Broderick, and R. Townsend, J. Chem. Soc. A **169**, 633 (1967).

[17] W. B. Kay and D. W. Hissong, Proc. Am. Pet. Inst., Div. Refin. **47**, 653 (1967).

[18] T. S. Akhundov and S. Y. Imanov, Teplofiz. Svoistva Zhidk. **12**, 48 (1970).

[19] A. M. Mamedov, T. S. Akhundov, and S. Y. Imanov, Russ. J. Phys. Chem. (Engl. Transl.) **44**, 877 (1970).

[20] D. Ambrose, J. Chem. Thermodyn. **19**, 1007 (1987).

[21] G. Christou, Ph.D. Thesis, University of Melbourne, 1988.

[22] R. D. Chirico, S. E. Knipmeyer, A. Nguyen, A. B. Cowell, J. W. Reynolds, and W. V. Steele, J. Chem. Eng. Data **42**, 758 (1997).

[23] T. S. Akhundov and N. N. Asadullaeva, Izv. Vyssh. Uchebn. Zaved., Neft Gaz. **11**, 83 (1968).

[24] R. J. Powell, F. L. Swinton, and C. L. Young, J. Chem. Thermodyn. **2**, 105 (1970).

[25] D. Ambrose, J. D. Cox, and R. Townsend, Trans. Faraday Soc. **56**, 1452 (1960).

[26] W. B. Kay and D. W. Hissong, Proc. Am. Pet. Inst., Div. Refin. **49**, 13 (1969).

[27] M. T. Raetzsch and G. Strauch, Z. Phys. Chem. (Leipzig) **249**, 243 (1972).

[28] L. C. Wilson, W. V. Wilding, H. L. Wilson, and G. M. Wilson, J. Chem. Eng. Data **40**, 765 (1995).

[29] R. D. Chirico, S. E. Knipmeyer, A. Nguyen, and W. V. Steele, J. Chem. Eng. Data **42**, 772 (1997).

[30] D. M. von Niederhausern, G. M. Wilson, and N. F. Giles, J. Chem. Eng. Data **45**, 157 (2000).

[31] E. D. Nikitin, A. P. Popov, N. S. Bogatishcheva, and Y. G. Yatluk, J. Chem. Eng. Data **47**, 1012 (2002).

[32] M. Frenkel, R. D. Chirico, V. Diky, C. D. Muzny, A. F. Kazakov, J. W. Magee, I. M. Abdulagatov, and J. W. Kang, *NIST ThermoData Engine*, *NIST Standard Reference Database 103b, Version 5.0* (National Institute of Standards and Technology, Standard Reference Data Program: Gaithersburg, MD, 2010).

[33] K. G. Joback and R. C. Reid, Chem. Eng. Commun. **57**, 233 (1987).

[34] P. J. Mohr, B. N. Taylor, and D. B. Newell, J. Phys. Chem. Ref. Data **37**, 1187 (2008).

[35] E. W. Lemmon and R. T. Jacobsen, J. Phys. Chem. Ref. Data **34**, 69 (2005).

[36] F. Neubeck, Z. Phys. Chem., Stoechiom. Verwandtschaftsl. **1**, 649 (1887).

[37] B. Woringer, Z. Phys. Chem., Stoechiom. Verwandschaftsl. **34**, 257 (1900).

[38] L. S. Kassel, J. Am. Chem. Soc. **58**, 670 (1936).

[39] K. S. Pitzer and D. W. Scott, J. Am. Chem. Soc. **65**, 803 (1943).

[40] C. B. Willingham, W. J. Taylor, J. M. Pignocco, and F. D. Rossini, J. Res. Natl. Bur. Stand. (U.S.) **35**, 219 (1945).

[41] A. F. Forziati, W. R. Norris, and F. D. Rossini, J. Res. Natl. Bur. Stand. (U.S.) **43**, 555 (1949).

[42] R. K. Nigam and B. S. Mahl, Indian J. Chem. **9**, 1250 (1971).

[43] M. Diaz Peña, A. Compostizo, and A. Crespo Colin, J. Chem. Thermodyn. **11**, 447 (1979).

[44] C. Castellari, R. Francesconi, and F. Comelli, J. Chem. Eng. Data **27**, 156 (1982).

[45] W. Hessler and W. Lichtenstein, Wiss. Z. Wilhelm-Pieck-Univ. Rostock, Naturwiss. Reihe **35**, 27 (1986).

[46] A. Aucejo, S. Loras, V. Martinez-Soria, N. Becht, and G. Del Rio, J. Chem. Eng. Data **51**, 1051 (2006).

[47] W. H. Perkin, J. Chem. Soc. **69**, 1025 (1896).

[48] O. Miller, Bull. Soc. Chim. Belg. **41**, 217 (1932).

[49] A. W. Francis, Ind. Eng. Chem. **49**, 1779 (1957).

[50] G. M. Panchenkov, T. S. Maksareva, and V. V. Erchenkov, Zh. Fiz. Khim. **32**, 2787 (1958).

[51] J. L. Hales and R. Townsend, J. Chem. Thermodyn. **4**, 763 (1972).

[52] T. S. Patterson, J. Chem. Soc. **81**, 1097 (1902).

[53] L. M. Heil, Phys. Rev. **39**, 666 (1932).

[54] L. Massart, Bull. Soc. Chim. Belg. **45**, 76 (1936).

[55] L. S. Shraiber and N. G. Pechenyuk, Russ. J. Phys. Chem. (Engl. Transl.) **39**, 219 (1965).

[56] A. M. Mamedov, T. S. Akhundov, and A. D. Tairov, Izv. Vyssh. Uchebn. Zaved., Neft Gaz **10**, 72 (1967).

[57] J. F. Skinner, E. L. Cussler, and R. M. Fuoss, J. Phys. Chem. **72**, 1057 (1968).

[58] T. S. Akhundov, Ph.D. Thesis, Baku, 1974.

[59]J. G. Hust and R. E. Schramm, J. Chem. Eng. Data **21**, 7 (1976).

[60]S. K. Garg, T. S. Banipal, and J. C. Ahluwalia, J. Chem. Thermodyn. **25**, 57 (1993).

[61]D. V. S. Jain, R. Chadha, and S. K. Sehgal, Fluid Phase Equilib. **96**, 195 (1994).

[62]A. Et-Tahir, C. Boned, B. Lagourette, and P. Xans, Int. J. Thermophys. **16**, 1309 (1995).

[63]N. Swain, D. Panda, S. K. Singh, and V. Chakravortty, J. Chem. Eng. Data **42**, 1235 (1997).

[64]G. Moumouzias, C. Ritzoulis, and G. Ritzoulis, J. Chem. Eng. Data **44**, 1187 (1999).

[65]G. Moumouzias and G. Ritzoulis, J. Chem. Eng. Data **45**, 202 (2000).

[66]N. Swain, S. K. Singh, D. Panda, and V. Chakravortty, J. Mol. Liq. **85**, 321 (2000).

[67]N. Swain, S. K. Singh, D. Panda, and V. Chakravortty, J. Mol. Liq. **94**, 233 (2001).

[68]H. Wang, L. Hu, and Y. Wu, J. Chem. Thermodyn. **27**, 1119 (2005).

[69]J. Chen, R. Shen, W. Liu, and G. Yu, J. Chem. Thermodyn. **39**, 934 (2007).

[70]T. Yang, S. Xia, S. Song, X. Fu, and P. Ma, J. Chem. Eng. Data **52**, 2062 (2007).

[71]R. Gonzalez-Olmos and M. Iglesias, Fluid Phase Equilib. **267**, 133 (2008).

[72]C. Y. Song, H. Z. Shen, J. H. Zhao, L. C. Wang, and F. A. Wang, J. Chem. Eng. Data **53**, 1110 (2008).

[73]A. K. Nain, P. Chandra, J. D. Pandey, and S. Gopal, J. Chem. Eng. Data **53**, 2654 (2008).

[74]J. A. Al-Kandary, A. S. Al-Jimaz, and A. H. M. Abdul-Latif, J. Chem. Eng. Data **51**, 2074 (2006).

[75]A. K. Nain, Phys. Chem. Liq. **45**, 371 (2007).

[76]A. K. Nain, Fluid Phase Equilib. **259**, 218 (2007).

[77]R. J. L. Andon, J. D. Cox, E. F. G. Herington, and J. F. Martin, Trans. Faraday Soc. **53**, 1074 (1957).

[78]J. D. Cox and R. J. L. Andon, Trans. Faraday Soc. **54**, 1622 (1958).

[79]I. A. Hossenlopp and D. G. Archer, J. Chem. Thermodyn. **20**, 1061 (1988).

[80]H. M. Huffman, G. S. Parks, and A. C. Daniels, J. Am. Chem. Soc. **52**, 1547 (1930).

[81]J. W. Williams and F. Daniels, J. Am. Chem. Soc. **46**, 903 (1924).

[82]D. V. S. Jain, R. Chadha, and S. K. Sehgal, Fluid Phase Equilib. **81**, 273 (1992).

[83]S. J. Park and J. Gmehling, J. Chem. Eng. Data **34**, 399 (1989).

[84]S. Malanowski, B. Zegalska, and B. Swiatek, Sel. Data Mixtures, Ser. A **22**, 313 (1994).

[85]R. D. Chirico, S. E. Knipmeyer, A. Nguyen, J. W. Reynolds, and W. V. Steele, J. Chem. Eng. Data **42**, 475 (1997).

[86]S. Didaoui-Nemouchi, A. Ait-Kaci, and J. Jose, Fluid Phase Equilib. **255**, 78 (2007).

[87]S. Uno, K. Kurihara, K. Ochi, and K. Kojima, Fluid Phase Equilib. **257**, 139 (2007).

[88]D. Tyrer, J. Chem. Soc., Trans. **105**, 2534 (1914).

[89]M. A. Azim, S. S. Bhatnagar, and R. N. Mathur, Philos. Mag. **16**, 580 (1933).

[90]D. R. Caudwell, Ph.D. Thesis, Imperial College, 2004.

[91]B. A. Grigor'ev, D. S. Kurumov, and S. A. Plotnikov, Russ. J. Phys. Chem. (Engl. Transl.) **57**, 130 (1983).

[92]J. S. Chang and M. J. Lee, J. Chem. Eng. Data **40**, 1115 (1995).

[93]J. S. Chang, M. J. Lee, and H. M. Lin, J. Chem. Eng. Data **41**, 1117 (1996).

[94]M. I. Aralaguppi, T. M. Aminabhavi, S. B. Harogoppad, and R. H. Balundgi, J. Chem. Eng. Data **37**, 298 (1992).

[95]R. Paramo, M. Zouine, and C. Casanova, Int. J. Thermophys. **24**, 185 (2003).

[96]R. Paramo, M. Zouine, F. Sobron, and C. Casanova, J. Chem. Eng. Data **51**, 123 (2006).

[97]J. H. Mathews, J. Am. Chem. Soc. **48**, 562 (1926).

[98]N. S. Osborne and D. C. Ginnings, J. Res. Natl. Bur. Stand. (U.S.) **39**, 453 (1947).

[99]M. E. Anthoney, A. S. Carson, and P. G. Laye, J. Chem. Soc., Perkin Trans. 2, 1032 (1976).

[100]J. L. San Jose, G. Mellinger, and R. C. Reid, J. Chem. Eng. Data **21**, 414 (1976).

[101]A. G. Osborn and D. R. Douslin, J. Chem. Eng. Data **19**, 114 (1974).

[102]A. Chianese and L. Marrelli, J. Chem. Eng. Data **30**, 424 (1985).

[103]G. Natarajan and D. S. Viswanath, J. Chem. Eng. Data **30**, 137 (1985).

[104]N. O. Smith, J. Chem. Eng. Data **35**, 387 (1990).

[105]F. J. Llopis and J. B. Monton, J. Chem. Eng. Data **39**, 643 (1994).

[106]H. Block, Z. Phys. Chem. Stoichiom. Verwandtschaftsl. **78**, 385 (1912).

[107]F. M. Jaeger, Z. Anorg. Allg. Chem. **101**, 1 (1917).

[108]T. W. Richards, C. L. Speyers, and E. K. Carver, J. Am. Chem. Soc. **46**, 1196 (1924).

[109]J. Timmermans and F. Martin, Travaux du Bureau International D'Etalons Physico-Chimiques **23**, 747 (1926).

[110]F. Fairbrother, J. Chem. Soc. 1846 (1934).

[111]A. Qin, D. E. Hoffman, and P. Munk, J. Chem. Eng. Data **37**, 66 (1992).

[112]M. Tasioula-Margari and I. N. Demetropoulos, J. Chem. Eng. Data **37**, 77 (1992).

[113]N. C. Exarchos, M. Tasioula-Margari, and I. N. Demetropoulos, J. Chem. Eng. Data **40**, 567 (1995).

[114]A. Konti, G. Moumouzias, and G. Ritzoulis, J. Chem. Eng. Data **42**, 614 (1997).

[115]T. Avraam, G. Moumouzias, and G. Ritzoulis, J. Chem. Eng. Data **43**, 51 (1998).

[116]J. M. Resa, C. Gonzalez, R. G. Concha, and M. Iglesias, Phys. Chem. Liq. **42**, 493 (2004).

[117]C. Yang, W. Xu, and P. Ma, J. Chem. Eng. Data **49**, 1802 (2004).

[118]Z. Di, P. Ma, S. Xia, and T. Yang, Petrochem. Technol. **35**, 851 (2006).

[119]E. Bich, K. Fiedler, G. Opel, and E. Vogel, Z. Phys. Chem. (Leipzig) **262**, 402 (1981).

[120]I. A. Hossenlopp and D. W. Scott, J. Chem. Thermodyn. **13**, 423 (1981).

[121]C. Yokoyama, S. Moriya, and S. Takahashi, Fluid Phase Equilib. **60**, 295 (1990).

[122]R. J. Corruccini and D. C. Ginnings, J. Am. Chem. Soc. **69**, 2291 (1947).

[123]J. F. Messerly, H. L. Finke, W. D. Good, and B. E. Gammon, J. Chem. Thermodyn. **20**, 485 (1988).

[124]J. B. Ott, J. R. Goates, and R. B. Grigg, J. Chem. Thermodyn. **11**, 1167 (1979).

[125]R. B. Scott and F. G. Brickwedde, J. Res. Natl. Bur. Stand. (U.S.) **35**, 501 (1945).

[126]F. R. Buck, K. F. Coles, G. T. Kennedy, and F. Morton, J. Chem. Soc. 2377 (1949).

[127]R. Dreyer, W. Martin, and U. Von Weber, J. Prakt. Chem. **1**, 324 (1955).

[128]C. P. Yang and M. Van Winkle, Ind. Eng. Chem. **47**, 293 (1955).

[129]P. Chaiyavech, J. Chem. Eng. Data **4**, 53 (1959).

[130]J. Kraus and J. Linek, Collect. Czech. Chem. Commun. **36**, 2547 (1971).

[131]E. W. Funk, F. C. Chai, and J. M. Prausnitz, J. Chem. Eng. Data **17**, 24 (1972).

[132]T. S. Akhundov, Izv. Vyssh. Uchebn. Zaved., Neft Gaz. **16**, 42 (1973).

[133]D. V. S. Jain and O. P. Yadav, Indian J. Chem. **12**, 718 (1974).

[134]T. S. Akhundov, S. Y. Imanova, and N. N. Bairamova, Izv. Vyssh. Uchebn. Zaved. Neft Gaz. **19**, 74 (1976).

[135]A. G. Osborn and D. W. Scott, J. Chem. Thermodyn. **12**, 429 (1980).

[136]Q. Zhao and V. N. Kabadi, J. Chem. Eng. Data **49**, 462 (2004).

[137]H. Matsuda, K. Yokoyama, H. Kyuzaki, K. Kurihara, and K. Tochigi, J. Chem. Eng. Jpn. **43**, 247 (2010).

[138]H. Landolt and H. Jahn, Z. Phys. Chem., Stoichiom. Verwandtschaftsl. **10**, 289 (1892).

[139]A. I. Vogel, J. Chem. Soc. (London) 607 (1948).

[140]M. Griffel, R. S. Jessup, J. A. Cogliano, and R. P. Park, J. Res. Natl. Bur. Stand. (U.S.) **52**, 217 (1954).

[141]G. M. Panchenkov and V. V. Erchenkov, Ukr. Fiz. Zh. (Russ. Ed.) **7**, 801 (1962).

[142]R. P. Singh, C. P. Sinha, J. C. Das, and P. Ghosh, J. Chem. Eng. Data **34**, 335 (1989).

[143]K. Chylinski and J. Gregorowicz, Fluid Phase Equilib. **64**, 237 (1991).

[144]R. Francesconi and F. Comelli, Thermochim. Acta **179**, 149 (1991).

[145]D. V. S. Jain, R. Chadha, and S. K. Sehgal, Fluid Phase Equilib. **112**, 151 (1995).

[146]J. George and N. V. Sastry, J. Chem. Eng. Data **48**, 977 (2003).

[147]C. Yang, P. Ma, and Q. Zhou, Chin. J. Chem. Eng. **12**, 537 (2004).

[148]Y. M. Naziev, A. N. Shahverdiyev, and V. H. Hasanov, J. Chem. Thermodyn. **37**, 1268 (2005).

[149]R. Gonzalez-Olmos, M. Iglesias, J. M. Goenaga, and J. M. Resa, Int. J. Thermophys. **28**, 1199 (2007).

[150]A. V. Korabel'nikov, Uch. Zap. Kursk. Gos. Pedagog. Inst. **51**, 144 (1971).

[151]V. Svoboda, V. Charvatova, V. Majer, and V. Hynek, Collect. Czech. Chem. Commun. **47**, 543 (1982).

[152]F. E. Blacet, P. A. Leighton, and E. P. Bartlett, J. Phys. Chem. **35**, 1935 (1931).

[153]R. H. Smith and D. H. Andrews, J. Am. Chem. Soc. **53**, 3644 (1931).

[154]N. D. Kolossowsky and V. V. Udovenko, J. Gen. Chem. USSR (Engl. Transl.) **4**, 1027 (1934).

[155]G. B. Guthrie, R. W. Spitzer, and H. M. Huffman, J. Am. Chem. Soc. **66**, 2120 (1944).

[156]T. S. Akhundov and C. I. Sultanov, Izv. Vyssh. Uchebn. Zaved. Neft Gaz **18**, 74 (1975).

[157]A. M. Mamedov, T. S. Akhundov, and C. I. Sultanov, Izv. Vyssh. Uchebn. Zaved. Neft Gaz **19**, 65 (1976).

[158]R. A. Andolenko and B. A. Grigor'ev, Iaz. Vyssh. Ucheb. Zaved., Neft i Gaz **22**, 78 (1979).

[159]E. W. Lemmon and R. T Jacobsen, J. Phys. Chem. Ref. Data **29**, 521 (2000).

[160]E. W. Lemmon, V. D. Arp, and D. O. Ortiz-Vega, "The Gruneisen parameter and fluid state equations" (unpublished).